Carbonaceous anode materials for lithium-ion batteries – the road ahead

T. Prem Kumar, T. Sri Devi Kumari AND A. Manuel Stephan

Electrochemical Power Systems Division, Central Electrochemical Research Institute, Council of Scientific and Industrial Research, Karaikudi 630006, Tamil Nadu, India

Abstract | Graphites and hard carbons are the mainstay of anode materials in practical lithium-ion batteries. With their dominance beginning to be threatened by other alternative anode materials such as silicon and intermetallics, continual research is directed at exploring known carbonaceous materials as well as at synthesizing new carbon-based anodes. After a review of lithium storage mechanisms in various carbon forms, this article explores avenues for crossovers between chemistry and materials science for tailoring carbonaceous materials that can cater to increasing power demands of emerging technologies. In particular, this review suggests opportunities and problem areas in anodes based on carbon composites as well as novel carbonaceous materials such as kish graphites, carbon nanotubes, nanofibers, curved carbon lattices and graphenes that are expected to prolong the legacy of carbon in lithium-ion batteries.

Keywords: Lithium-ion battery; lithium intercalation; graphite; carbonaceous anodes; carbon nanostructures

1. Introduction

Carbon is unique in that an entire branch of chemistry is based on its compounds. That elemental carbon also plays a major role in human civilization in myriad but inconspicuous ways often escapes our attention: diamonds for jewellery and abrasives, carbon fibers as reinforcement material in tennis racquets, activated carbons for deodorization, decolorization and water purification, carbon blacks for inks, carbon-resin composites for speakers, carbon membrane switches in electronic gadgets, graphite electrodes in electrochemical industries, carbon arc electrodes in projectors, leads in pencils, etc. One of the most recent applications is as anode in lithium-ion batteries. In fact, the success story of present-day lithium-ion battery technology rests largely on one anode: carbon [1]. Since 1990 when Sony Energytec unveiled the lithium-ion technology [2], carbon has continued to be the mainstay of anode materials for lithium-ion batteries. Carbonaceous materials as negative electrodes in lithium-ion batteries possess desirable features such as higher specific charges and lower redox potentials than other candidate materials (metal oxides, chalcogenides and polymers) in addition to better cycling behaviour than lithium-alloying elements [3].

Unlike competing secondary battery systems such as the versatile lead-acid battery, which is 150 years old, lithium-ion batteries are of recent origin [2]. Yet they have established a niche market especially for powering portable electronic gadgets such as cellular phones, PDAs, laptops, etc., which demand small and light batteries with short charging times [4]. Lithium-ion batteries are also ideally suited for use in space-limited gadgets that require power packs to occupy voids between electronic components or even line the inside of the gadget's body. Such flexible designs can be envisaged in implantable devices, smart cards, rolled-up displays and RFID tags. Apart from the higher energy densities they possess (Fig. 1) as compared to competing systems such as the nickel-cadmium and nickel metal hydride batteries [5], lithium-ion batteries also offer a broader temperature range of operation and a lower self-discharge

Memory effect is a term used to describe a self-conditioning phenomenon by which nickel-cadmium cells tend to adjust their electrical properties to a certain duty cycle to which they have been subjected to for extended periods of time. It results in a temporary loss in capacity when nickel-cadmium cells are subjected to (a) a large number of unvarying partial discharge-charge cycles (generally to not more than 40% of depth of discharge); (b) extended storage without recharge or without sufficient charge; and (c) prolonged constant-current charging. The temporary loss in capacity means that the cells deliver less capacity than they are designed for. Memory effect is a reversible phenomenon observed in cells with sintered-type cadmium negative electrodes.

Figure 1: Potentials and charge densities of candidate anode materials. On the right are presented salient features of the lithium-ion battery technology.

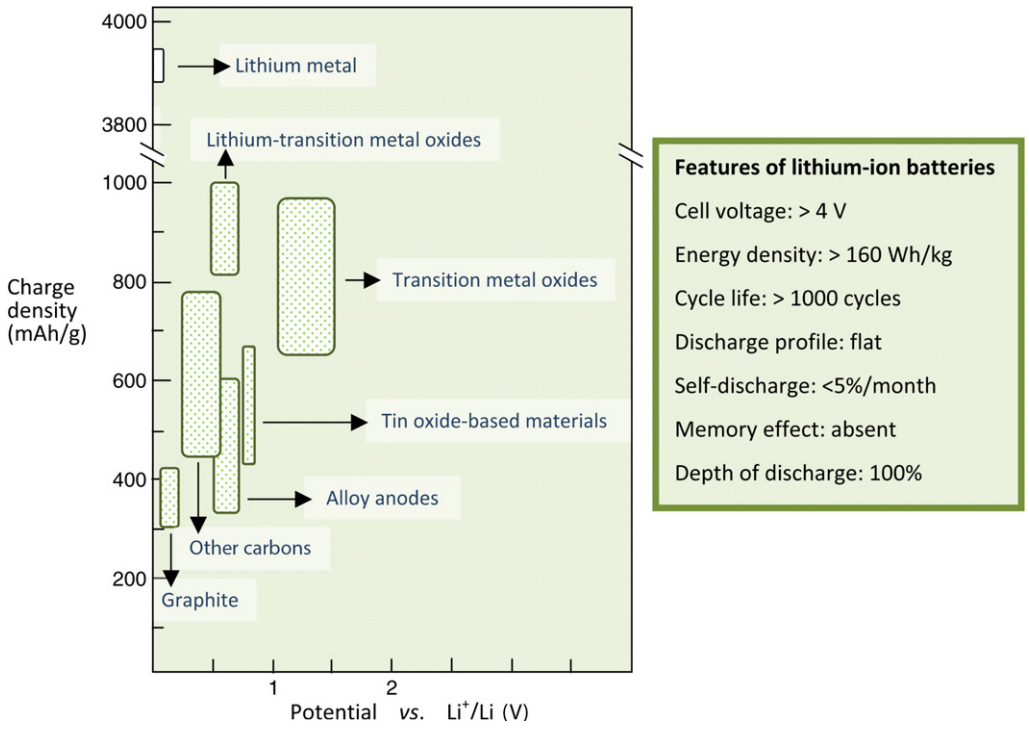

An insertion reaction (opposite: extrusion) is a general term given to a chemical reaction or transformation in which a guest atom, molecule or ion is introduced into a host crystal lattice. An intercalation reaction is a specific term given to an insertion reaction in which the host material undergoes no major structural changes; intercalation reactions are generally reversible insertion reactions in which the guest species occupy positions pre-determined by the structure of the host material. We also come across topotactic/topochemical reactions, which are reversible or irreversible reactions in which the insertion of a guest species into a host structure results in significant structural modifications to the host (e.g., breakage of bonds). Thus, intercalation and topotactic reactions are subsets of insertion reactions.

rate. They also do not suffer from memory effect [6]. Today, the lithium-ion battery represents the cutting edge of human knowledge in terms of the science and technology of electrochemical power systems; yet burgeoning demands for higher energy densities for applications such as electric traction raises the performance bar towards the upper right side in Fig. 2. Such developmental goals must also be consistent with the need for safety, high-rate capability, low-temperature performance and cyclability [7].

SEI is a passivation film formed by reaction of the electrode material with the electrolyte. This film is electronically insulating, but is a good conductor of lithium ions. It prevents direct contact between the electrode and the electrolyte, suppressing further reaction between them [8].

1.1. *The lithium-ion battery*

Before we go into a discussion on carbonaceous anode materials, let us familiarize ourselves with the working of the lithium-ion battery. The lithium-ion battery is a lithium-ion transfer cell in which lithium ions shuttle between two lithium intercalation/insertion electrodes. Lithium ions move from the cathode to the anode during charge and back to the cathode during discharge (Fig. 3). Common candidates for the cathode are lithiated metal oxides, while carbon is the most popular anode material. This reversible transfer of lithium ions to and from interstitial sites in the host materials is accompanied by charge transfer. Ionic transport within the cell is ensured by an aprotic organic electrolyte, usually a solution of $LiPF_6$ in high-permittivity, low-viscous solvent mixtures made from alkyl carbonates such as ethylene carbonate, diethyl carbonate and dimethyl carbonate. The longevity of the system is ensured, among other things, by a solid-electrolyte interphase (SEI) on the surfaces of the electrodes. Lithium-ion batteries do not employ lithium metal as the anode. The lithium-ion battery is, therefore, often described as a lithium metal-free lithium battery.

2. Carbons for lithium storage

Carbon as an insertion anode material was first proposed in 1973 [9]. Carbonaceous materials have large variations in crystallinity, chemical composition and microtexture depending on their preparation, processing, precursor, and thermal and chemical activation treatments. In fact, all carbonaceous materials are capable of storing lithium, although the amount and nature of lithium accommodation depends on a combination of several factors such as mechanical milling [10], structure and crystallinity [11], particle size [12], surface area [13], surface species [14,15], and even the binder [16] and composition of the electrolyte

Figure 2: Gravimetric and volumetric energy densities of common battery systems.

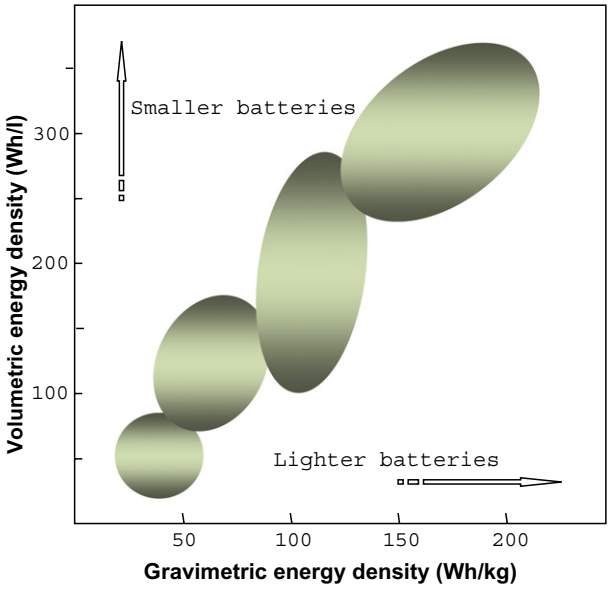

[17,18]. The identification of a long-cycling, high-capacity carbon anode for lithium-ion batteries must, therefore, wait for a holistic understanding of the effect of several structural and morphological characteristics on the reversible insertion processes in a variety of electrolyte solutions.

Carbons investigated for their lithium insertion properties include graphites, cokes, mesophase pitches, carbon fibers and whiskers, glassy and vitreous reticulated carbons, pyrolytic carbons, buckminsterfullerenes and carbon nanotubes. Doped and chemically modified carbons have also been investigated. Graphitic carbons are characterized by layers of hexagonally arranged carbon atoms in a planar condensed ring system called graphene layers. Graphites, both natural and synthetic, support reversible intercalation of lithium ions at potentials close to that of lithium. In its fully lithiated state, LiC_6, a perfectly graphitic material can give a capacity of 372 mAh/g. Graphite's popularity as an anode material is also underpinned by facile kinetics for reversible lithium intercalation. The reversible capacity of graphite materials can be raised by improving their degree of crystallinity

Figure 3: A schematic of the working principle of the lithium-ion cell.

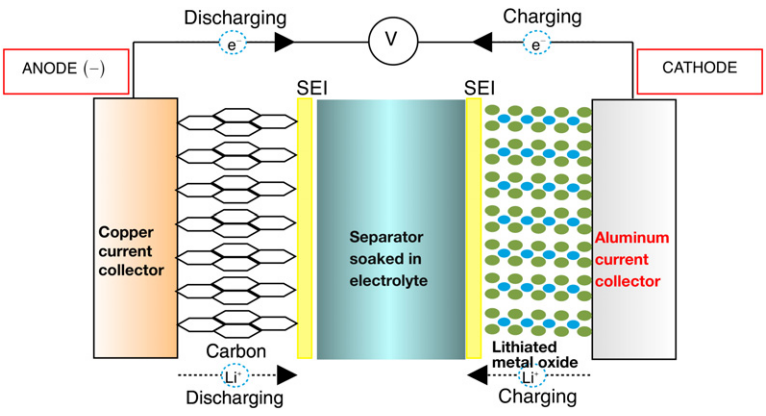

Figure 4: Graphene stacks in graphitizable and non-graphitizable carbons.

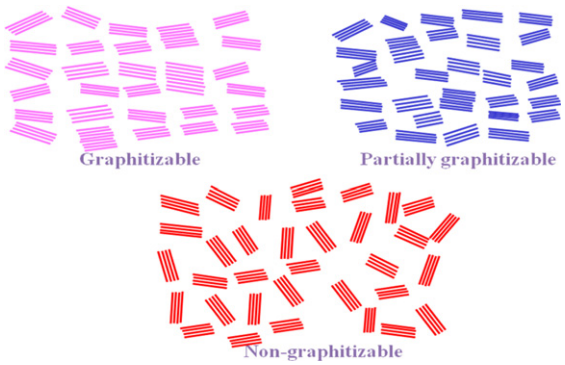

[19,20]. A flake-like morphology, due to its high degree of graphitization, is known to favour high reversible capacities, although this advantage is compromised by reduced cyclability and rate capability [21]. Fiber morphologies bestow good long-term cyclability and high-rate capability to graphites. It must be mentioned in passing that there is no direct correlation between practical values of gravimetric and volumetric energy densities [21]. Carbon nanotubes are also graphitic materials, but present a variety of storage sites, which account for higher lithium insertion capacities [18,22]. The utility of carbon nanotubes in lithium-ion batteries is dictated among other things by their structure, wall thickness and surface area. They are often used as additives to improve cyclability [18,23]. Disordered carbons (carbons with no long-range crystalline ordering) possess appealing features like high uptake of lithium and excellent cyclability [24–28]. However, large irreversible capacities and hysteresis limit their exploitation [29,30]. According to some authors, the performance of hard carbons is good when their crystallinity is low and are rich in small pores [31,32]. However, Azuma *et al.* [33] suggest that large capacities may be realized by (i) enhancing the 'adsorbing force' of pseudo-metallic lithium atoms and (ii) reducing the 'repulsion force' between doped lithium atoms in the carbon matrix.

2.1. *Graphitic and non-graphitic carbons*

Carbonaceous materials are generally classified as graphitic and non-graphitic carbons. Perfectly layered graphitic carbons can store lithium between hexagonal graphene sheets: one lithium for every six carbon atoms (LiC_6), which corresponds to a specific charge of 372 mAh/g. Lithium intercalation in these carbons occurs at potentials near the reduction potential of metallic lithium. Non-graphitic carbons also have a hexagonal network of carbon atoms, but lack long-range ordering. Non-graphitic or disordered carbons can be further classified as soft and hard carbons depending on whether or not they graphitize upon heat treatment between 1500 and 3000°C (Fig. 4). Hard carbons, typically those with an H/C atomic ratio of less than 0.1, can store higher amounts of lithium than graphitic carbons [34]. However, the voltage profiles of soft carbons show appreciable hysteresis (about 1 V) during charge/discharge cycling. On the other hand, hard carbons do not show hysteresis during charging and discharging.

2.2. *Lithiated graphite*

The interlayer space in graphite can accommodate certain atoms, ions and even molecules to give products called graphite intercalation compounds (GICs) [35]. Insertion is possible even in carbon materials with partially developed graphite structures such as those with small crystallite sizes along both *a* and *c* axes. In such cases, the use of the term graphite intercalation compound is rather inappropriate. GICs can be divided into two categories depending on the type of bonding between the host planes and the intercalate. For example, in graphite oxide and graphite fluoride, where the bonding is covalent, the bonding alters the layer structure into tetrahedrally coordinated carbons. Since there are no conduction electrons, these compounds are insulators. In the second category, the bonding is ionic where atomic or molecular layers of a different chemical species are inserted between carbon layers along the *c*-axis of the hexagonal graphite lattice [36,37]. The latter category GICs can be subdivided into two groups depending on the guest species: electron-accepting intercalates such as Br_2, $FeCl_2$, $SbCl_5$, TiF_4 and $TiOF_2$ forming *p*-type conductors, and electron-donating intercalates such as alkali metals forming *n*-type conductors [38]. The charge balance in these compounds is realized through the formation, respectively, of macrocations C_n^+ and macroanions C_n^- [39].

Electrochemical intercalation of lithium from aprotic solutions into graphite to form Li-GICs is accompanied by reduction of graphite. Similarly, Li-GIC is oxidized upon deintercalation. The reactions can be described by the following equation:

$$6C + Li^+ + e^- = LiC_6 \qquad (1)$$

When the anode is charged, lithium ions from the solution get intercalated into the carbon host; upon discharge, lithium ions deintercalate and enter the electrolyte. Upon intercalation, the graphite layers slide in order to accommodate the

Figure 5: Top: Lithium intercalated graphite, showing lithium ions between graphene layers. Bottom: In-plane distribution of lithium in Li_xC_6.

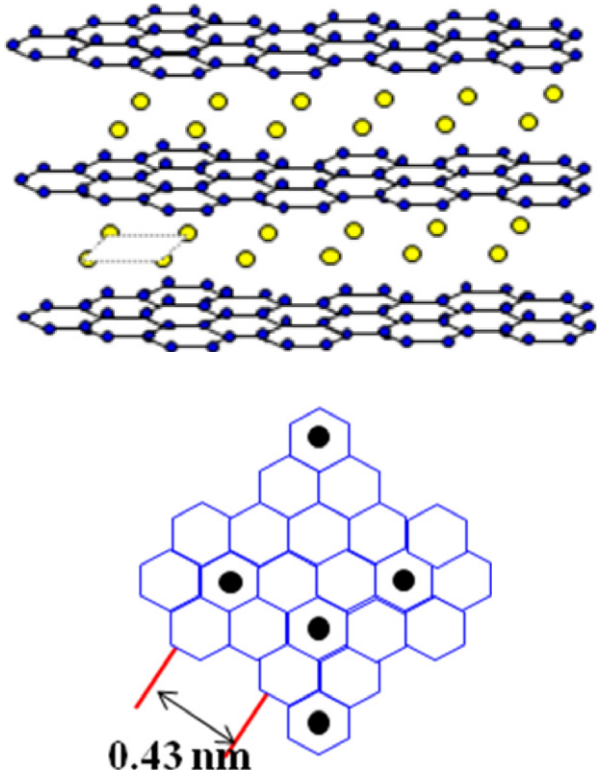

Zintl phase is a term applied to intermetallic compounds that have a strong polar bonding component. By general definition, it is a class of materials between intermetallic and ionic compounds, formed by a metal from group 1 or 2 with a heavier post-transition metal or metalloid from groups 13, 14 or 15 in the Periodic Table. Zintl phases are strongly ionic and are brittle in nature.

Staging is a phenomenon by which graphite intercalation compounds form regularly stacked structures in which galleries of intercalated species are separated by a fixed number of graphene layers. For example, in stage-I compound, single layers of graphene alternate regularly with single layers of the intercalated species. Similarly, in a stage-II compound, two layers of graphene separate two successive layers of the intercalant.

intercalant: the *A–B–A–B* registry of the hexagonal carbon planes in the graphite gets changed into an *A–I–A–I–A* stacking order so that the intercalant, *I*, occupies the site between two basal planes of eclipsed hexagons formed by six carbon atoms in the graphite layer (Fig. 5) [40]; simultaneously, the interlayer distance expands from the original 3.354 Å to 3.71 Å [41]. The reversibility of this reaction is the key to the success of carbon as an anode in lithium-ion cells.

^{7}Li-NMR studies by Tatsumi *et al.* [42,43] showed that the oxidation state of the intercalated lithium was +1. In fact, these authors found that the Knight shift of lithium species in Li-GICs nearly matched that of LiCl at all intercalation levels. The absence of metallic lithium species in Li-GICs suggests a mere transfer of lithium ions between the electrolyte and the carbon host during the charge-discharge processes, justifying the nomenclature "lithium-ion battery." However, conventional wisdom has it that electrode reactions in a galvanic cell must be accompanied by oxidation/reduction. Accordingly, it is suggested that during charging, the guest lithium ion accepts an electron from the outer circuit and gets reduced to metallic lithium. Subsequently, the lithium atom donates that electron to the carbon host, which forms macroanions of the formula C_n^-. This is akin to the Zintl phases observed in lithium-aluminum alloys [44,45]. During the discharge process, lithium ions get into the electrolyte with a simultaneous release of electrons from the host carbon into the outer circuit.

GICs possess physical and chemical properties quite different from those of graphite [46]. For example, some GICs show such high electrical conductivity that they are proposed as alternatives to metallic conductors [47,48]. GICs possess desirable properties for use in galvanic cells: they can have electroactive species in electronic contact with the graphite matrix; they are insoluble in the battery electrolyte; they are conductive both in the charged and discharged states*; and they are mechanically stable with respect to cycling.

*Highly oriented pyrolytic graphite (HOPG-.∞) has a *c*-direction conductivity, σ_c, of is 8.3 S/cm [49]. Its in-plane conductivity, σ_a, is three orders higher, with $\sigma_a/\sigma_c = 3000$ [49]. The σ_c of LiC_6, the stage-I Li-GIC, is 1.8x10^4 S/cm [50]. For LiC_6 $\sigma_a/\sigma_c = 14$ [50], which means that conductivity is less anisotropic in LiC_6 than in graphite.

Figure 6: Galleries of lithium ions in different stages of Li-GICs.

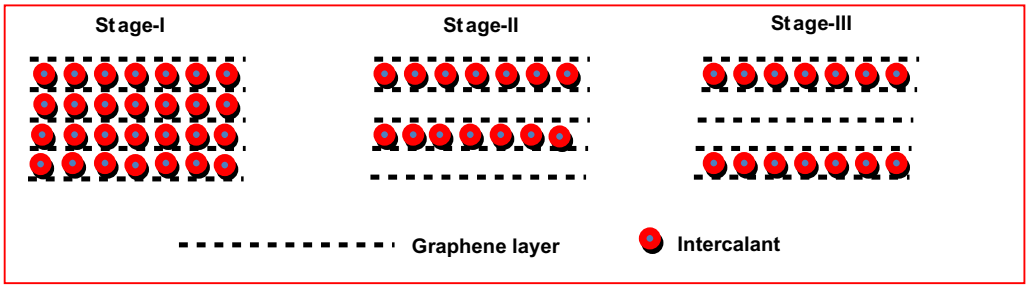

Battery researchers use the symbol C to denote the rated capacity of a cell or battery. The capacity of a battery is expressed in ampere-hours (Ah), which is a multiple of the current output/input in amperes and the duration in hours of discharge/charge. The charging and discharging current of a cell is often expressed as a multiple of C. For example, the 0.1C current for a cell with a rated capacity of 4 Ah is 400 mA. In theory, a current of 100 A can be drawn for 1 hour from a 100-Ah battery (C rate); alternatively, 1 A can be drawn from it over 100 hours (C/100 rate).

3. Graphitic anodes

With a theoretical capacity of 372 mAh/g, corresponding to the stage-I compound LiC_6 (Fig. 6), graphite, usually artificial graphite, has remained a popular choice for the anode in lithium-ion batteries [51]. Natural graphite as an alternative is not only less expensive, but also exhibits higher capacities, up to 15% more than those of artificial graphites, owing to their higher degree of graphitization [52]. Although the energy density of lithium-ion batteries based on graphite has been increasing by about 10% annually [53], the onslaught from competing anode materials has remained unabated. However, given its availability, low cost and satisfactory lithium insertion behaviour, tremendous effort is being expended on identifying novel forms of carbons that can satisfy materials needs of next-generation anodes in lithium-ion batteries. By careful optimization of particles and pore structure, Yishi *et al.* [54] developed an artificial graphite that gave a practical specific capacity of 360 mAh/g with 95% charge–discharge efficiency. The new material also could sustain high discharge rates. The development of new graphitic anodes requires heat treatment at temperatures around 3000°C, which makes processing energy-intensive and often calls for management of evolving gaseous products. Therefore, much attention is focused on natural graphites. Su *et al.* [55] used a three-dimensional graphitic carbon in order to improve the rate capability of graphite. The new material, a macroporous carbon with a surface area of around 42 m^2/g and an interconnected pore structure consisting of 30 nm-thick graphitic walls synthesized by using inverse silica opal as a template and benzene vapour as the carbon precursor, yields a specific capacity of 326 mAh/g at a current density of 40 mA/g. The material also displays good high-current performance, with a capacity of 303 mAh/g at 600 mA/g. Three-dimensional amorphous carbons with similar structures prepared by templating techniques fare poorly compared to this graphitic carbon [56,57].

3.1. *Kish graphites*

Since the serendipitous discovery of carbon nanostructures in graphites produced by catalytic graphitization from iron melts supersaturated with carbon [58], kish graphites have begun to be noted as a new anode material. These are highly graphitic materials (degree of graphitization: ~92% [58]) and are silken to the touch. In Fig. 7 are presented typical SEM images of kish graphites, showing their characteristic flaky morphology. Kish graphites have been demonstrated to exhibit lithium insertion capacities well above the theoretical value of 372 mAh/g that can be tapped from perfectly graphitic structures [59,60]. The 'excess' capacity is attributed to the presence of a variety of carbon nanostructures embedded in this material (Fig. 8). A hallmark of this material is a low first-cycle irreversible capacity, which was just 14% in one study [59]. Kish graphites also sustain extended cycling with coulombic efficiencies touching 100%. The production of this graphite variety is rather inexpensive and involves relatively low temperatures of around 1500°C. Furthermore, the structure of kish graphites can be modified by use of suitable inoculants, opening up a whole new avenue of investigation. Some of our recent results with bismuth as an inoculant has shown steady capacities of about 380 mAh/g over the 200 cycles at C/10 rate that the material has sustained till the time of submitting this article (Fig. 9) [61].

4. Disordered carbons

As lithium insertion materials, disordered carbons possess several desirable features [52,62–64]: high lithium storage capacities, often much higher than the theoretical limit of 372 mAh/g that perfectly graphitic structures can offer; (ii) possibility of introducing structural and compositional variations by varying the nature of precursors and temperature protocols; and (iii) good cycling ability. Disordered carbons obtained by pyrolysis of organic precursors

Figure 7: SEM images of kish graphites showing their characteristic flaky morphology.

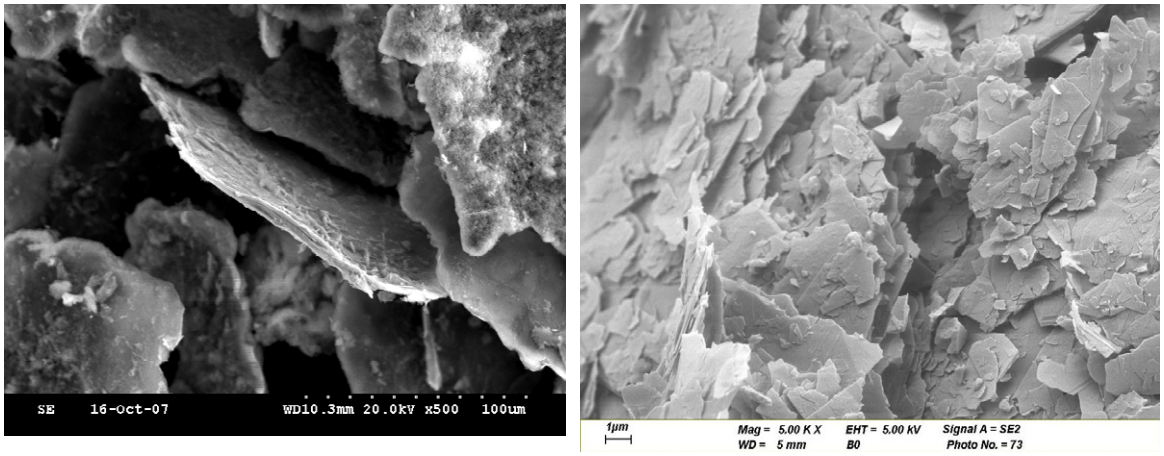

Figure 8: SEM images of kish graphites showing a variety of nanostructured carbons.

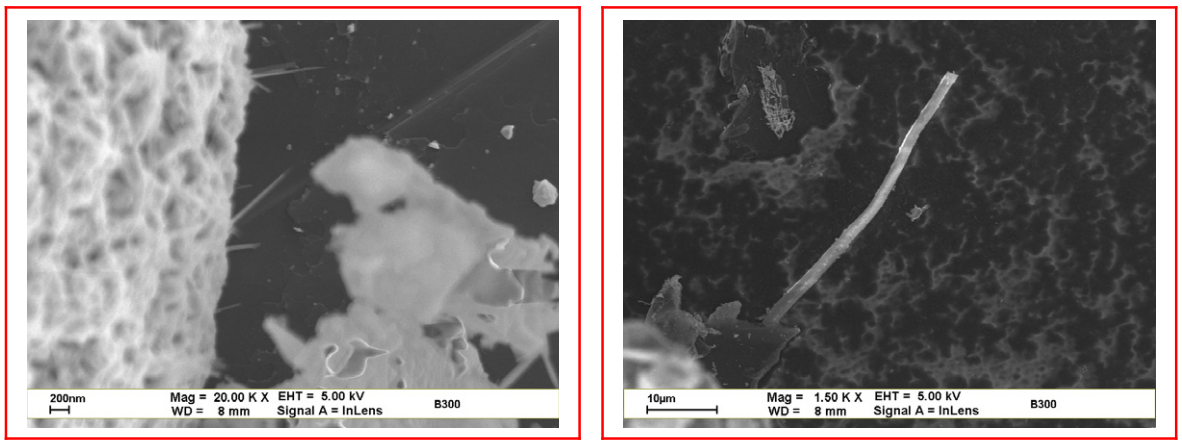

contain a predominantly planar hexagonal network of carbons, but lack extended crystallographic ordering. Pyrolytic carbons have also been known to retain up to 30 at.% of residual hydrogen [52,65,66]. The high lithium storage capacities of these carbons are related to both disorder [67,68] and hydrogen content [52,64,69]. The absence of long-range order frustrates attempts at understanding the relationship between the structure and reversible lithium insertion properties of disordered carbons. Despite their large insertion capacities, the applicability of these carbons in practical cells is hampered by large irreversible capacities, and polarization between charge and discharge (hysteresis) (Fig. 10). While irreversible capacity loss would mean use of extra mass of cathode material to compensate for this loss, the hysteresis would lower the coulombic efficiency.

4.1. *Lithium storage in disordered carbons*

The fact that different carbon varieties can store different amounts of lithium suggests that lithium storage in carbons can occur by more than one mechanism. Soft carbons are known to contain substantial quantities of hydrogen, which saturate the dangling bonds of the edge carbon atoms, forming polyaromatic hydrocarbons [69]. It has been shown that the extent of hysteresis is proportional to the hydrogen content. According to Dahn *et al.* [52] lithium accommodation occurs at sites near the hydrogen atoms and that it would alter the C–H bonding, leading to hysteresis. The

Figure 9: Cycling behaviour of a typical kish graphite at C/10 rate between 3.000 and 0.005 V.

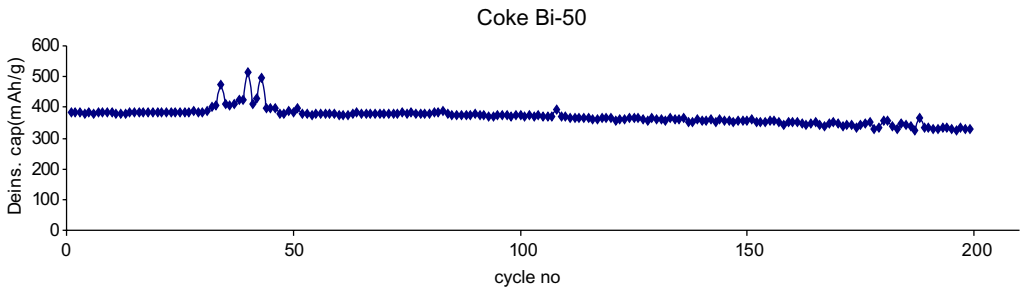

large hysteresis is attributed to (H–C)–Li bridging, in which a two-coordinated edge carbon with a hydrogen would transform from the sp^2 to the sp^3 hybridized form [70,71]. Yata *et al.* [62,63], who investigated polyacenic semiconductors (PAS) as lithium-insertion anodes, found that the specific charge increases with increasing H/C atomic ratio. ^{7}Li NMR studies with lithiated PAS materials showed that lithium ions were less tightly bound in PAS than in LiC_6, with no specific interaction between the hydrogen and the lithium nuclei [72]. Lithium storages up to a stoichiometry of LiC_2 were achieved with PAS materials by a mechanism that did not involve formation of lithium clusters [72]. In another ^{7}Li NMR study, Sato *et al.* [65] suggested the formation of dilithium molecules (Li_2) in disordered carbons. Given the strong repulsion between lithium ions, the possibility of such diatoms has been questioned. In a recent paper, however, Ishikawa *et al.* [73], based on binding energy calculations, showed that Li_2 could indeed exist (see below).

Figure 10: Charge-discharge profiles of graphitic and disordered carbons.

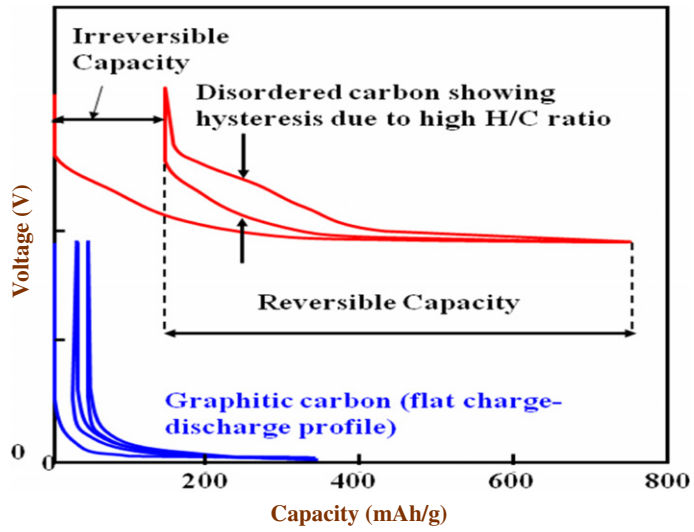

Papanek *et al.* [69] showed that lithium atoms could occupy both edge and interstitial sites up to LiC_3 composition. They proposed bonding of lithium atoms to edge carbons of aromatic hydrocarbon molecules [69], with a local geometry similar to the organo-lithium molecule $C_2H_2Li_2$ [74]. According to the authors, the energies of the edge sites and the interstitial sites were nearly the same; they suggested that lithium insertions at both the sites would, therefore, occur at the same potential [69]. Based on their *ab initio* calculations, Ago *et al.* [75] showed accommodation of lithium at both hydrocarbon edges and interstitial sites. According to Ishikawa and co-workers [73], the binding of lithium in carbons is associated with substantial negative binding energies. Based on their first principles calculations, these authors showed binding energies of −142.8 kJ/mol for pyrenes, −211.0 kJ/mol for anthracenes and −146.2 kJ/mol for phenanthrenes [73]. The possibility of the existence of Li_2 was suggested in anthracene and phenanthrene in which the binding energies are −200.5 and −146.2 kJ/mol, respectively, being larger in magnitude than the dissociation energy for Li_2 [73]. With the accommodation of lithium ions, the host lattice loses its planarity, the distortion facilitating stronger interaction between the host and the guest species.

As noted earlier, the lithium storage capacity of graphite is limited by lithium accommodation of one "ion" site for every six sp^2 hexagonal carbon (LiC_6). Sato *et al.* [65] proposed an Li_2 covalent molecule model in disordered carbons, with capacities of up to 1116 mAh/g (LiC_2). Other authors have suggested a variety of other accommodation sites including both

sides of graphene sheets, nanovoids, etc. in order to explain high capacities [76–78]. Disordered carbons, characterized by a predominance of single, unaligned and buckled carbon layers as well as nanopores and nanovoids, present a variety of sites for lithium accommodation [68,79–82]. Lithium may also locate on the zigzag and arm-chair faces of individual layers [76,83]. However, disordered carbons also exhibit large irreversible capacities. According to Mabuchi *et al.* [79,80] lithium accommodated in nanopores present between unorganized carbon sheets is often difficult to retrieve. The irretrievability of inserted lithium and passivation processes on the large surface areas provided by the carbons contribute to the irreversible capacity.

Low-crystallized carbons can be prepared from natural and synthetic organic precursors that form a fluid phase during pyrolysis under inert gas. The structure of pyrolytic carbons is generally related to the structure of the precursors [84]. For example, sugars yield hard carbons. On the other hand, coal tar pitches yield soft carbons, graphitization of which is facilitated by a strong tendency of carbon-containing moieties to self-assemble in the mesophase intermediate formed during pyrolysis. A notable example is the carbonization of hexabenzocoronene, a molecular graphene [85]. Carbons obtained from condensed aromatics and carbon-rich polymers such as poly-paraphenylene [86], polyacenic materials [62,63], acrylonitrile-butadiene-styrene terpolymer [87], hexa(phenyl)benzene [86,87], polyacrylonitrile [27,28] and 3,4,9,10-perylene-tetracaboxylic acid-dianhydride [89] have shown capacities of up to 700 mAh/g. Natural precursors include starch and oak [32], walnut and almond shells [32], peanut shells [90], rice husk [26], banana fibers [91], lignin, cotton and wool [92], and sugar [32,93–97]. Fey *et al.* [90] demonstrated initial lithium intake of as much as 4765 mAh/g for porogen-treated pyrolytic carbons obtained from peanut shells. However, the high irreversible capacities and continued loss in capacity with cycling hamper their exploitation in high-energy lithium-ion batteries.

Figure 11: Spider wedge model of the constituent molecules in mesophase pitch [101,102].

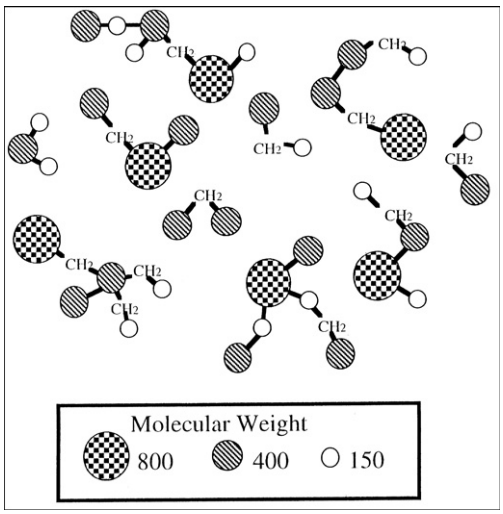

5. Other carbon forms

5.1. *Mesophase pitch-based carbons*

The sheer variety of forms in which carbon manifests itself is truly amazing. Among precursors that can generate such a complexity of structures are coal and coal tar pitch. For example, simple heat treatment of coal and coal tar pitch can give rise to anisotropic spheres, believed to be nematic liquid crystals that consist of aromatic oligomers in which aromatic planes are stacked nearly parallel to each other [98]. Hot-stage microscopic studies revealed that anisotropic graphitizable coke can be produced through several successive steps, finally yielding bulk mesophase by coalescence of anisotropic (mesophase) spheres [99,100]. The structure of the constituent molecules, described by a spider wedge model, is illustrated in Fig. 11 [101]. Here, aromatic units of diameter 0.6–1.5 nm are joined by phenyl–phenyl linkages or methylene bridges, yielding substances with molecular weights ranging between 400 and 4000. Mochida *et al.* [102] compared the electrochemical lithium insertion behaviour of mesophase pitches derived by heat-treatment of aromatic hydrocarbons (Fig. 12). Although such materials are potential candidates for anode in lithium-ion batteries, much needs to be understood in terms of their irreversible capacity and cyclability. The presence of a variety of aromatic ring systems opens up opportunities for the preparation of hard carbons with pre-designed structures and heteroatoms.

5.2. *Templated carbons*

Because a predictable control over critical properties such as surface area and porosity would aid in better designing carbons for higher performance, some groups attempted custom synthesis of carbons. For example, Sandi *et al.* [81,103] used pillared clays with known inter-planar spacings as templates for the synthesis of carbons. Specifically, a synthetic carbon fiber prepared by using sepiolite as a template gave a lithium insertion capacity of 633 mAh/g [104]. These fibers were found to be microporous in

Figure 12: Discharge profiles of mesophase pitch products: graphitized mesophase-based carbon fiber (3000°C); hard carbon prepared from oxidized naphthalene isotropic pitch (1000°C); and soft carbon prepared from naphthalene mesophase pitch (700°C) [101].

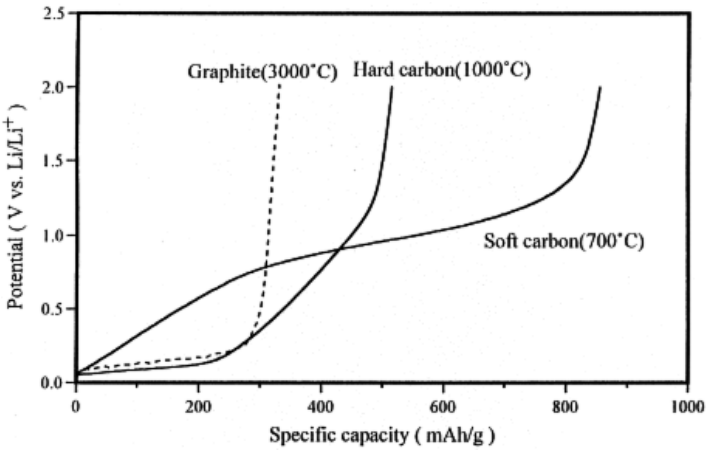

nature, with a mean pore radius of 6.8±0.5 Å, which means that in terms of molecular dimensions they have a curvature similar to that of the corannulene molecule [105]. As we shall see later in this review, the reversible lithium capacities of corannulene and the fiber are similar, suggesting that the curvature of carbon surfaces do play a role in lithium storage.

Similar templated porous carbons have drawn much attention as promising materials for lithium storage. Often their improved capacity is offset by large irreversible capacities arising out of their high surface areas. Meyers *et al.* [106] employed K-10 montmorillonite clay, Y, Beta and ZSM-5 zeolites as inorganic templates in which suitable organic precursors were carbonized. Among precursors employed for template synthesis are acrylonitrile, furfuryl alcohol, pyrene, and vinyl acetate. However, the microporous products exhibited no significant capacity.

Figure 13: Rate performance of hierarchically porous carbon samples obtained at different temperatures and non-porous carbon carbonized from mesophase pitch without template at 700°C [107].

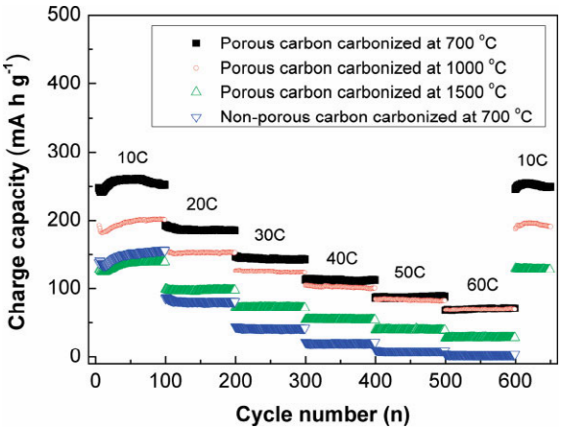

Among the highest reversible capacities reported for a carbon material is an ordered mesoporous carbon (average pore size: 3.9 nm) prepared from sucrose with ordered silica as a template [56]. The product gave an initial deinsertion capacity of 3,100 mAh/g between 0.1 and 0.5 V *vs.* Li^+/Li. This corresponds to an unprecedented composition of $Li_{8.4}C_6$ for the lithiated carbon. In the subsequent cycles they obtained reversible capacities ranging from 850 to 1100 mAh/g. The good performance is attributed to the ordered nanoporous structure of the material. In another report, a carbon with a three-dimensional network of mesopores and micropores was obtained by carbonizing mesophase pitch in a monolithic silica template [107]. At C/5 rate, the hierarchically porous product gave a first-cycle capacity as high as 900 mAh/g, which stabilized at around 500 mAh/g after 15 cycles. What is noteworthy about this material is its high-rate capability. As Fig. 13 shows, it gave 540 mAh/g at C rate, 260 mAh/g at 10C rate, 145 mAh/g at 30C rate and 70 mAh/g at 60C rate [107]. The excellent rate performance is a result of the favorable transport characteristics of this hierarchically porous carbon structure. The unique structure provides an efficient mixed conducting three-dimensional network: while the well-interconnected carbon wall structure provides a continuous electronic pathway, the network of pores facilitates electrolyte diffusion into the bulk of the electrode material, enhancing lithium ion transport. Moreover, the large surface area of the material leads to a high electrode/electrolyte contact area with a large number of active sites for charge transfer. The rate capability is also related to the wall thickness, which is of the order of a few tens of nanometers, greatly reducing the solid-state transport lengths for lithium ion diffusion. A similar work by Su *et al.* [55] was further proof of the improved high-rate performance and cyclability of such structures. Carbons with such high rate capability are sure answers to emerging high-power applications.

5.3. *Polyacenic semiconductors*

PAS-based anodes prepared by pyrolysis of phenol-formaldehyde resins have inter-layer distances between 3.7 and 4.0 Å [108,109]. Considering that the inter-layer distances in graphite and LiC_6 are 3.35 Å [110] and 3.70 Å [108], respectively, the inter-layer distance in PAS provides easy accessability to

Figure 14: Charge and discharge curves of (a) PAHs and (b) PAS. Current density: 0.5 mA/cm^2 [34].

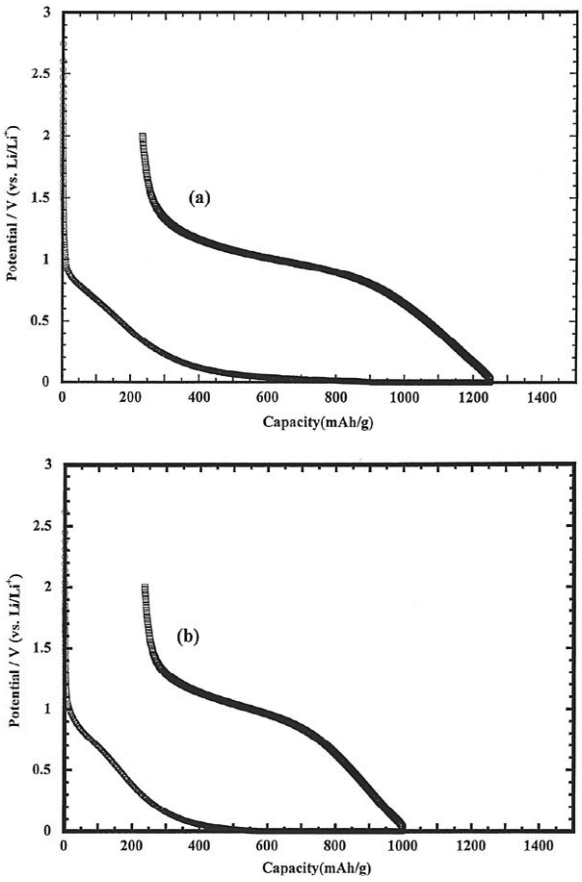

Li^+ ion, whose radius is 0.6 Å [110]. PAS materials can be doped with electron acceptors and electron donors, with the products exhibiting an 11-order increase in electrical conductivity [111]. Yata *et al.* [62,63] demonstrated a capacity of 530 mAh/g as well as good stability and cyclability with PAS materials. Although the sloping discharge profile and large hysteresis in their charge-discharge curves limit their applicability, synthetic carbons with graphite-like structures have evoked much interest. Among similar materials investigated are graphite-like pyropolymers with relatively high electrical conductivity derived by pyrolysis of polymers or by high-temperature polycondensation reactions. Suh *et al.* [112], who prepared carbons from black polyacene-based polymers, showed reversible lithium insertion capacities of 496 mAh/g with poly[(*Z*)-1-methoxy-4-phenyl-1-buten-3-yne].

5.4. *Polycyclic aromatic hydrocarbons*

Carbonaceous materials such as PAS with H/C atomic ratios of 0.2–0.4 are high-capacity lithium insertion anodes [62,63]. One study reports a pyrolyzed PVC product (H/C = 0.36) with a reversible capacity of 940 mAh/g [113]. In another study, Takami and co-workers [114] demonstrated a capacity of 804 mAh/g for a perylene-based disordered carbon (H/C = 0.26). Unfortunately, their first-cycle irreversible capacities were 25–35%. Wang *et al.* [34] reported a polycyclic aromatic hydrocarbon (PAH) material made from isotropic pitch with a capacity of 1017 mAh/g and efficiency of 81.5% (Fig. 14). Wang *et al.* [34] proposed models for graphene sheets in PAHs and PASs, representing them in disc-like and ribbon-like configurations. According to them PAHs have small graphene sheets and weak cross-linking between neighboring crystallites so that the carbon at the edge of the graphene sheet can accept significant amounts of lithium, accounting for the large capacities [34]. Bonino *et al.* [25] synthesized hexa(phenyl) benzene via a Diels–Alder cycloaddition starting from tetraphenyl cyclopentadiene and diphenylacetylene. Carbon obtained by pyrolysis of the product gave an initial deinsertion capacity of more than 1,000 mAh/g, which stabilized around 550 mAh/g over the 100 cycles reported. What is unique here is that unlike other disordered carbons, whose capacity fades progressively with cycle number, the hexa(phenyl) benzene-derived pyrolytic carbon exhibited a steady capacity (around 550 mAh/g), which is a feature that can be exploited for high-performance lithium-ion batteries.

PAHs, described above, are typical molecular graphenes [115] (diameter less than 5 nm along the 2D direction of graphene) with all the carbons in the sp^2 hybridized state. PAHs have precisely defined structures and tunable solubility. They are amenable to processing and can be prepared in bulk. If such structures can be extended to produce macrographenes by bottom-up chemical synthesis, it would widen the scope of carbonaceous materials for lithium storage. Apart from the PAHs (two-dimensional polyphenylenes), other unconventional carbon structures such as polyphenylene dendrimers (three-dimensional polyphenylenes) and combinations thereof may add to the variety of carbon-based electronic materials [116]. Zhi and Mullen [115] have reviewed chemical approaches to grow PAHs into larger graphenes. According to them thermolytic methods with carbon-rich precursors, such as smaller PAHs, followed by reactions at high temperatures to fuse or grow the PAHs into larger graphenes would be versatile ones [115]. The procedure is also convenient for template-assisted integration of molecular graphenes into unconventional carbon nano-objects.

It is interesting to note that oligophenylenes cannot be indefinitely planarized; in fact, beyond a limit they begin to fold, yielding partially closed three-dimensional structures [117]. Such novel two-dimensional and three-dimensional giant graphite segments hold promise as lithium storage materials. For example, three-dimensional graphitic materials prepared by controlled solid-state pyrolysis of well-defined carbon-rich phenylene molecules such as hexaphenylbenzene and hexa(4-bromophenyl)benzene gave capacities of the order of 600 mAh/g [25,86]. Formation of such structures is facilitated by intermolecular aryl-aryl and intramolecular cyclodehydrogenation reactions [25,118].

5.5. *Curved carbon lattices*

A totally novel approach to carbons with high lithium storage capacity is based on the concept that carbons with curved lattices can accommodate larger amounts of lithium than do graphite. The idea is underscored by computational studies of endohedral complexes of lithium with buckminsterfullerene, C_{60} [119]. According to Scanlon and Sandi [119,120] the interior of the C_{60} molecule is not only large enough to accommodate two or three lithiums, but also has a curvature that facilitates close approach of lithium. In fact, the inter-lithium distance of 2.96 Å in the trilithiated species is smaller than that in LiC_6 (4.25 Å [121]), which suggests that it is possible to realize lithium insertion capacities exceeding 372 mAh/g with carbons that have curved lattices that approximate a portion of the C_{60} molecule [122]. Corannulene, $C_{20}H_{10}$ (Fig. 15), has a bowl-shaped geometry in which none of the five six-member carbon rings are coplanar with the others [123]. In fact, the structure of corannulene resembles a curved section of a buckeyball [124]. Corannulene has been shown to give a reversible lithium insertion capacity of 602 mAh/g [125]. Geodesic structures such as corannulene could be the next big thing in carbon-based anodes for lithium-ion batteries. However, this presupposes that the synthesis of such buckybowls will become commercially feasible. From 1966, when corannulene was first synthesized by a 17-step process with yields of just a few milligrams [126], we have already come a long way in that today it is possible to synthesize 25-gram batches of the compound by a simple solution-based procedure [127]. Given the tremendous efforts being taken towards assembling buckyballs from bowl-shaped constituents, it is not too far fetched to imagine the production of buckyballs with a hole or two in it, allowing reversible insertion of hundreds of milliampere-hours equivalent of lithium.

6. Carbon nanostructures

Nanostructures present novel properties associated with decreased size, unique shape and defects, and have been demonstrated to exhibit characteristics often superior to their bulk counterparts [128–130]. For example, the rate capability of electrode materials is related to the rate of solid-state diffusion of lithium ions in the materials [131–137]. Use of nanoparticulate materials can mitigate the problem of slow diffusion by limiting the diffusion distance to the radius of the nanoparticle. Carrying forward this concept, lithium intercalation in carbon nanostructures such as fullerenes and carbon nanotubes (CNTs) [138–141] as well as one-, two- and three-dimensional carbon architectures [55,142–144] is increasingly being explored.

6.1. *Fullerenes and carbon nanotubes*

Historically, fullerenes preceded carbon nanotubes as a subject of research in lithium storage in line with the fact that they were discovered prior to carbon nanotubes. Fullerenes can enter into two types of doping: endohedral and exohedral. In the former the dopant resides on the inside of the fullerene shell, whereas in the latter it is present between fullerene molecules. Obviously, endohedral doping is associated with high activation energies. Electrochemical lithiation of C_{60} fullerenes can be achieved up to five electrons per molecule [145]. However, because the fulleride anion is soluble in the liquid electrolyte, Chabre *et al.* [146] used a polymer electrolyte and showed that a maximum of one lithium per five carbons could be injected into C_{60}, corresponding to $Li_8(Li^+)_4C_{60}^{4-}$, with eight lithium in neutral state [147]. Studies have also shown higher lithium intake by hydrogenated fullerenes $C_{60}H_x$ ($x < 60$) and $C_{70}H_x$ ($x < 70$) [148]. Like in hydrogen-containing disordered carbons, lithium uptake was found to be dependent on the degree of hydrogenation of the fullerenes [148].

That lithium insertion through the walls or the capped ends of CNTs is energetically not favourable was shown by Kar *et al.* [149], who investigated lithium insertion into CNTs by *ab initio* and DFT methods. For a defect-free CNT, lithium ions preferred a distance of around 1.9 Å from the tubewall. Based on their first principles simulation study, Meunier *et al.* [150] proposed lithium insertion through topological defects containing at least nine-sided rings and through open ends. Thus, nanotubes damaged by either chemical or mechanical means would yield materials with substantial lithium storage capability. Liu *et al.* [151], who used first principles molecular orbital calculations to study the energetics of lithium absorption by single-walled carbon nanotubes

Figure 15: Two-dimensional and three-dimensional structures of corannulene.

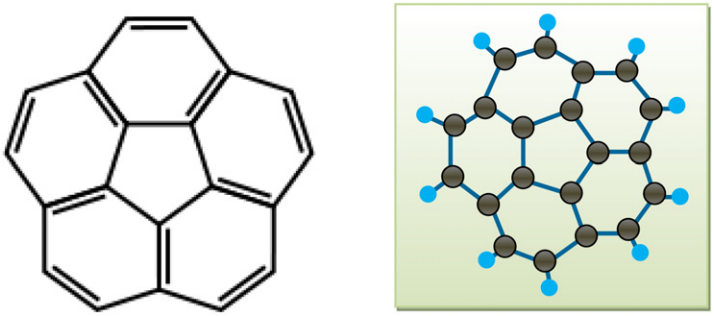

(SWCNT) as a function of tube diameter, showed that while the energy for lithium absorption on the outer wall decreased, it increased with increasing tube diameter for lithium absorption on the inner wall. However, the absorption energies for both sides of the walls tended to become similar for diameters larger than 0.824 nm.

Industry enthusiasts projected CNTs as high-performance anode materials due to their unique structure capable of supporting improved kinetics, and large surface area and high porosity that can provide additional lithium storage sites [134,152–155]. Theoretical calculations suggest that apart from the normal mode of lithium storage as Li_xC_6, an additional curvature-induced lithium condensation is a possibility inside the core of the nanotubes [156,157]. Such studies also show a linear dependence of the storage capacity on the diameter of CNTs [156,157]. Zhao *et al.* [158] and Meunier *et al.* [150] predicted the possibility of realizing lithium-rich compositions of Li_2C_6 or higher ($> 1,116$ mAh/g) with SWCNTs. Indeed practical capacities of more than 1,000 mAh/g were reported with SWCNTs [18,159–163]. Multi-walled carbon nanotubes (MWCNTs) are particularly attractive for additional reasons of possessing a variety of lithium accommodation sites: spacings between the graphite layers, local turbostratic disorders arising from their highly defective structures, and the central core. Studies have shown lithium intake of 100–1,400 mAh/g in CNTs [154,163–165]. The large capacities are often ascribed to defects and to a reduction in the length of the nanotubes, which can improve lithium diffusion properties [166]. Investigations on cycled CNTs have revealed that the structural integrity of the nanotubes remains unaffected by repeated lithium insertion, a property that promises long service life to batteries that use them [167,168]. Other advantages of CNTs are their appreciable electrical conductivity (10^{-4} S/cm), which can enable high power output from electrodes that use them; high thermal conductivity (2,000–4,000 W/mK), which can ensure good heat dissipation, and, therefore, improved safety of the device; and high strength, which can result in durable electrodes.

Carbons that have roughly parallel graphite layers of relatively small lateral extents of about 20–50 Å, but with random rotations and translations between every pair of layers are said to possess turbostratic disorder [140].

CNTs allow themselves to be processed into flexible free-standing paper-like electrodes without use of a conductive additive, metal substrate or binder. Ng *et al.* [168,169] used simple vacuum filtration to prepare bucky paper electrodes. Although their capacities were slightly lower than those of conventional electrodes, the bucky paper electrodes were lighter due to absence of substrate and binder. Moreover, the simple procedure keeps manufacturing costs low. In comparison to the filtration method, other approaches to thin film electrodes such as direct deposition of CNTs on metal substrates [170,171] or on carbon [172] and transfer of CNTs on to a layer of conducting polymer composite [173] are both cumbersome and expensive.

Electrodes with free-standing SWCNTs exhibited insertion capacities in the 400–460 mAh/g range [159,167,174,175]. Because of their large surface areas and mesoporous volume, there is considerable loss of lithium due to formation of SEI [174]. However, it is interesting to note that unlike graphite (which undergoes exfoliation in propylene carbonate-based electrolytes [176–178], SWCNTs gave improved performance with propylene carbonate-containing electrolytes, delivering a first-cycle reversible capacity of 520 mAh/g [179]. Due to its low melting point, propylene carbonate is a desirable constituent in low-temperature electrolytes. Thus, the good performance of CNTs in propylene carbonate-based electrolytes suggests the possibility of realizing CNT-based batteries that can operate at low temperatures.

Investigations have also been made on arrays of aligned carbon nanotubes (ACNT) in order

to produce highly ordered, high surface-area electrodes with excellent electronic and mechanical properties. Such arrays must be mechanically robust and sufficiently conducting in the horizontal direction. In a recent breakthrough, Chen *et al.* [173] used a conducting polymer composite layer that ensured both electrical connectivity and mechanical robustness. The composite layer is so thin that 90% of the CNT length is exposed, allowing the CNTs to perform a variety of functions, including lithium storage. Aligned MWCNTs produced by pyrolysis of iron(II) phthalocyanine [180] on a quartz plate were given a 100-nm thick coating of poly(3,4-ethylenedioxythiophene) (PEDOT) by chemical vapour pyrolysis. PEDOT ensured good electronic connectivity of the individual nanotubes. A second coating of 500 nm of poly(vinylidene fluoride) (PVdF) bestowed the necessary mechanical stability. The resulting flexible CNT array electrode could be peeled-off the quartz substrate without damage. The conductivity of the free-standing array electrode was over 200 S/cm. A lithium-ion battery assembled with this array anode gave a stable discharge capacity of 265 mAh/g over 50 cycles. However, it exhibited a rather high irreversible capacity (due to extensive SEI formation on its high-area surface). A significant improvement accruing from the use of this electrode is that it renders the use of a copper current collector superfluous [181]. The absence of copper substrate means that the weight of a typical CNT array electrode would be as small as 2 mg compared to 14 mg for one that uses a copper substrate [182]. Another advantage is the long-term stability of the electrode free from impurities released by copper dissolution in the electrolyte. The study provides a new strategy towards lightweight, flexible, highly conductive and mechanically robust rechargeable batteries.

Templated carbon nanotubular assemblies have also been of interest to battery scientists. Martin *et al.* [183] prepared free-standing carbon nanotubule membranes by chemical vapor deposition combined with anodically formed aluminium oxide. The nanotubule membranes delivered a capacity of 490 mAh/g. The authors also reported a tube-in-tube carbon membrane that gave at least twice the capacity [183]. The large capacities of the template-directed nanotube assemblies are attributed to their typical morphological features [143].

Reports of lithium insertion in CNTs with different features continue to appear in the literature. For example, ropes of SWCNTs have been reported to exhibit reversible capacities between 450 and 500 mAh/g [159,184]. There is at least one report which claims that mechanical milling of SWCNT bundles results in capacities of 1,000 mAh/g due to a shortening of the CNTs as well as to the introduction of defects [166]. Shimoda *et al.* [185] showed that chemical etching doubled the deliverable capacity of SWCNTs (700 mAh/g). The authors ascribed the enhanced capacity to diffusion of lithium into the interior of the SWCNTs through the opened ends and sidewall defects. It is known that lithium insertion through CNT sidewalls is energetically forbidden [186], for which reason accessing the interiors through surface defects and open ends could be an option. In fact, SWCNT samples deliberately made defective resulted in anodes with capacities nearing 1,000 mAh/g [184,187,188]. Wang *et al.* [189] subjected CNTs to mild oxidation between 300 and 450°C and obtained capacities of up to 533 mAh/g at a current density of 20 mA/g, a considerable increase over that of as-grown CNTs, which yielded only 305 mAh/g. The improvement was ascribed to the oxidation of reducing groups on the carbon surface as well as to a partial purification of the CNT product. Eom *et al.* [190] etched MWCNTs in a 3:1 mixture of concentrated H_2SO_4 acid HNO_3, and demonstrated reversible and irreversible capacities of 681 and 1229 mAh/g, respectively, for the product. Etching generated chemical and structural changes in the nanotubes, which enhanced the reversible capacity. The large irreversible capacity was suggested to be due to SEI formation on the large surface area of the etched product.

Similar to attempts at using heteroatom-incorporated carbons, boron-doped carbon fibers [191,192] and MWCNTs [139] have also been investigated. Zhou *et al.* [193,194] investigated the lithium insertion behaviour of boron- and nitrogen-doped SWCNTs using first-principles calculations. They showed that boron as a dopant dramatically decreased the lithium absorption energy on both the inner and outer walls by forming an electron-deficient carbon matrix, which could stabilize the absorption by accepting electrons from the absorbed lithium. However, nitrogen as a dopant formed an electron-rich structure, which would hinder lithium absorption because the structure cannot accept electrons from the absorbed lithium [193,194]. Mukhopadhyay *et al.* [139] realized 180 mAh/g with boron-doped MWCNTs, a slight increase from the 156 mAh/g observed with the undoped MWCNTs. Boron doping leads to a breakdown in the in-plane hexagonal symmetry of the walls [139,195,196] and to an increase in the electrical conductivity [195–198], features that might be exploited towards a good-performance anode. Nitrogen-doped MWCNTs, generated from pyridine as a precursor, was shown to reversibly insert lithium to an equivalent of 340 mAh/g [199].

Figure 16: Schematic representation of lithium insertion into and deinsertion from bamboo-shaped carbon nanofibers. The green and red dots represent reversible and irreversible lithium ions [208].

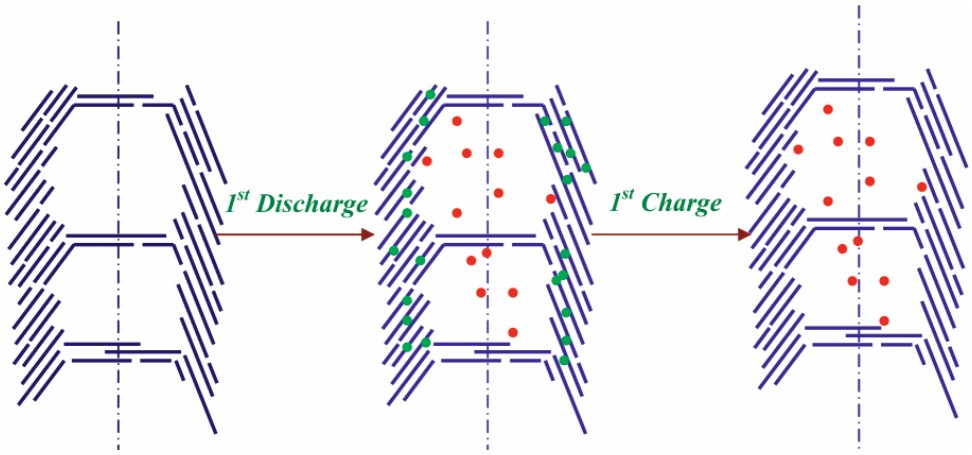

Ink-bottle effect is a pore-blocking effect observed with porous materials that have ink-bottle type pores. A simple description would be a large cavity fitted with a narrow cylindrical neck. Normally, pores in a sample are not directly connected to the surface or through larger pores. Thus, intrusion into the wide inner space will occur only if sufficient energy is supplied to force a species into the narrow openings. Because of the small neck of the pores, retrieval of the forced-in species is often incomplete. This leads to an intrusion–extrusion hysteresis and an associated entrapment of the inserted species. The ink-bottle effect has wide ramifications as in the analysis of data on mercury porosimetry and solvent evaporation from porous solids.

One disadvantage of using CNTs is that the lithium insertion behaviour of CNTs vary by a large measure by the type of the CNTs. Their utility will depend on reproducible production of identical CNTs. The first-cycle irreversible capacities are also often too large to merit practical applicability. The large hystereis between the charge-discharge potentials is another disadvantage. With several applications demanding a cycle life of more than 1,000 cycles, the capacity fade of CNT-based anodes upon cycling, especially for materials with high initial capacities, needs to be restrained [200].

6.2. *Carbon nanofibers*

Nanofibers, especially those with peculiar morphological features, have attracted attention as high-capacity anodes [201–203]. In fact, some of the carbon nanotubes being investigated actually qualify as carbon nanofibers because they lack in long-range ordering as in graphitic materials and/or they have imperfectly rolled graphene sheets. An advantage of carbon fibers is that unlike in defect-free carbon nanotubes, which permit lithium insertion only through open ends, lithium ions can also get inserted through surface defects in the fiber walls. Deng *et al.* [204] obtained a first-cycle lithium storage capacity of 682 mAh/g and a deinsertion capacity of 234 mAh/g with carbon nanofibers having periodic dome-shaped interiors. The large irreversible capacity was attributed to lithium trapped in void or cavity sites by the so-called ink-bottle effect [205–207].

Subramanian *et al.* [208] demonstrated high lithium storage capacities and high-rate capability with bamboo-shaped carbon nanofibers having structural and surface defects (Fig. 16). Reversible capacities of 461 mAh/g at 0.1C rate and 170 mAh/g at 10C rate were demonstrated with these fibers (Fig. 17). They attributed the good performance to mixed features of graphitic and disordered carbons in the fibers as well as to considerable reduction in the diffusion length for lithium ions [208].

Recently, Cho *et al.* [209] obtained a highly crimped nanofibrillar carbon from a polyacrylonitrile/$FeCl_3$ hybrid precursor. This material exhibited a reversible capacity of 630 mAh/g with a coulombic efficiency of about 70%. Moreover, in the voltage range between 0.06 and 0.80 V, the new material gave 100% efficiency for the lithium insertion reaction, yielding a capacity of about 400 mAh/g. Cho *et al.* [209] speculated that the excellent performance characteristics of the material had to do with its highly entangled web-like hyperstructure, which not only promoted easy permeation but also provided high resilience to volume deformation during the insertion/deinsertion processes. Habazaki *et al.* [210,211] synthesized carbon nanofilaments by liquid-phase carbonization using anodized aluminium oxide membrane templates. However, their reported capacities for the filaments prepared at elevated temperatures were inferior, which they ascribed to loops at the edge of graphene layers impeding deep intercalation of lithium. It was also reported that narrow filaments exhibited better rate capability, although their initial irreversible capacity was large [210,211]. The better rate capability was due to reduced diffusion lengths while the high irreversibility was due to easy platelet exfoliation and subsequent formation of an SEI film.

Figure 17: Cycling performance of carbon nanofibers at different C rates [208].

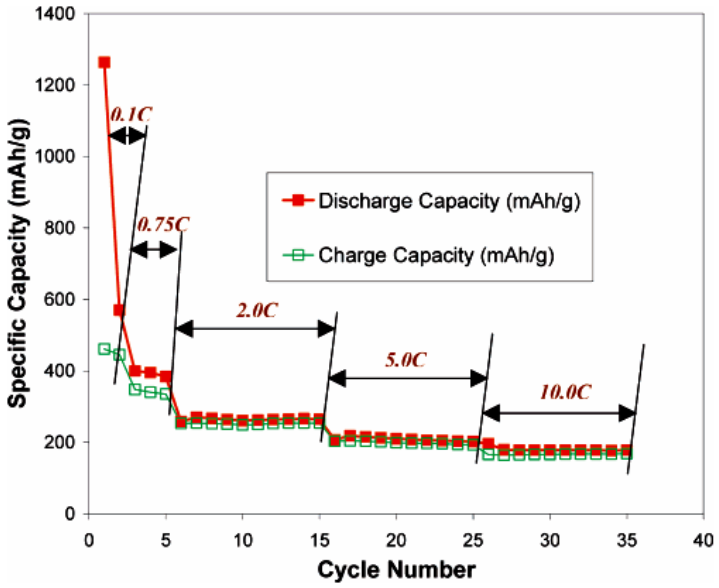

6.3. *Carbon nanocapsules*

Hollow carbon spheres or carbon capsules are a promising class of materials due to their good electrical conductivity, chemical inertness and controllable surface properties [212–216]. Su *et al.* [217] prepared smooth hollow spheres with carbon shells and nitrogen-doped shells by chemical vapour deposition using silica spheres obtained by a Stober process as templates. The graphitic nature of the shells was enhanced by raising the temperature of deposition. Both the materials exhibited good lithium-insertion behaviour, sustaining capacities slightly lower than 350 mAh/g at C/5 rate, and delivering more than 200 mAh/g at 15C rate. The good rate capability of the capsules, found to be better than that of a commercial sample of mesophase carbon microbeads, was attributed to better lithium diffusion characteristics offered by the open carbon network of the shell structure [218]. Su *et al.* [217] showed a relatively better performance with the nitrogen-doped carbon capsule, which they ascribed to the beneficial role of nitrogen in the graphene sheets of the sample [219,220]. However, these materials are unlikely to be of much commercial interest given their high cost of production and their relatively low specific capacities.

6.4. *Graphene-based anodes*

The strictly two-dimensional nanocarbon, graphene, is particularly interesting as a lithium storage anode. It is electrically conductive, mechanically robust, non-toxic, chemically and thermally tolerant, and has a large electrochemical stability window. A report by Levasseur *et al.* [221] describing the possibility of using graphite multi-layer thin films as lithium-insertion materials can be considered as a forerunner to graphene-based anodes. The thin films were prepared by a deposition process from a dispersion of graphite. The thin film assembly occurs by repeated substrate-induced coagulation that yields a porous network of agglomerated, well-crystallized graphite particles. Despite the apparent disorder of the small particles, the large ones get preferentially aligned, parallel to the substrate surface, forming a lamellar substructure.

Graphene prepared by solution chemistry routes lends itself to easy functionalization, which permits its assembly into functional nanostructures such as paper and thin films. Yata *et al.* [62] suggested that high capacities are possible with lithium covalently bonded as a dimeric molecule only if the interlayer spacing in carbons is large (~4.0 Å). In fact, graphene nanosheets with a large interlayer spacing ($d_{002} \sim 4.0$ Å) have been shown to store lithium equivalent to 740–780 mAh/g [222]. However, this value of capacity is larger than that of pyrolytic graphene oxide nanosheets (580 mAh/g) with similar d_{002} values [223]. This suggests the presence of other lithium storage sites such as vacancies and disorders believed to be generated in graphene during its preparation [224–227]. Recently, Pan and co-workers [228] obtained exceptionally high reversible capacities of 794–1054 mAh/g with graphene containing deliberately generated defects. Yoo *et al.* [222] doped graphene nanosheets with carbon nanotubes or C_{60} fullerene in order to enlarge the space between graphene layers. These structures exhibited larger capacities (730–784 mAh/g) than graphene nanosheets (540 mAh/g). The authors attributed the large capacities to the large d_{002} spacings (4 Å) in the doped materials [222].

The most obvious impediment to commercial exploitation of graphene materials for lithium-ion batteries is the absence of reliable methods for large-scale production of processable graphene sheets. The top-down approach of generating graphene by mechanical exfoliation of highly oriented pyrolytic graphite [229] and the bottom-up approach by heat treatment of silicon carbide wafers [230] apply only for fundamental studies that require very small quantities. An alternative top-down approach that holds promise involves oxidation of graphite [231–234], which unfortunately introduces defects in the product due to formation of oxygen-containing groups. Commercially viable synthetic strategies

must be explored in order to translate laboratory findings into devices.

In an attempt towards a scalable method for the production of graphene nanosheets, Murugan *et al.* [235] used a microwave-assisted solvothermal route to reduce exfoliated graphite oxide to produce 'chemically modified graphene nanosheets.' They also decorated the product with polyaniline and made a composite that gave a reversible capacity of about 800 mAh/g at C/15 rate with a capacity retention of 84% after 40 cycles.

7. Doped carbons

Heteroatom-doped carbons have also been of interest as anode materials [236–239]. The effect of heteroatoms on the lithium insertion properties of carbons has been discussed on the basis of electronic [240,241] and steric effects [242,243] although much remains to be understood especially because reports often have claims that seem to contradict one another [219,241].

7.1. *Boron-doped carbons*

Being of comparable size, boron as a substituent in a carbon lattice should not cause much distortion in the crystal structure. Moreover, boron with an electron less than carbon should act as an electron acceptor, creating a hole-carrier in the valence band, and thereby enhancing electrical conductivity and discharge capacity of carbon [244]. Boron incorporation also can enhance the degree of graphitization of graphites [245–247]. According to Lowell, the incorporation of boron in graphite is substitutional and not interstitial [248], a finding vindicated by the results of Dahn *et al.* [249,250], who investigated B_xC_{1-x} films. Dahn *et al.* [11,238] reported that lithium intercalation capacity of chemical vapour deposited boron-doped graphites was proportional to the boron content up to a composition of $Li_{1.16}(B_{0.17}C_{0.83})_6$. However, lithium intercalation occurs at 1.6 V *vs.* Li^+/Li, which was attributed to the electron-accepting nature of boron in the carbon lattice [251,252]. Several other investigators have probed the lithium insertion behaviour of boron-doped carbons such as pitch-derived graphite [253], mesophase pitch-based carbon fiber [254] and coke-derived graphites [255]. Tanaka *et al.* [256] showed that boron-doped pitch coke-derived graphite gave a capacity of 315 mAh/g as compared to a boron-free sample, which gave only 265 mAh/g (Fig. 18).

Figure 18: Second-cycle discharge curves B-0 (boron-free), B-5 (3.8% B) and B-10 (10.3% B) graphites. 0–3 V; 1.56 mA/cm^2 [256].

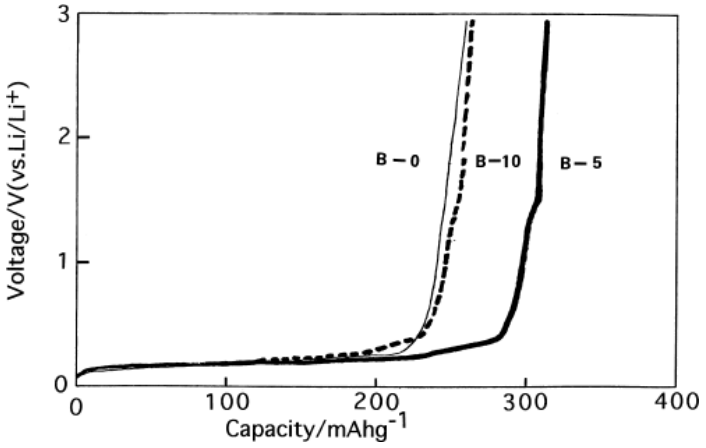

7.1.1. *Boron-doped diamond*

A relatively new material that has come to be investigated for lithium storage is boron-doped diamond [257,258]. Incorporation of boron creates a defective carbon lattice and enhances sp^2 character. Ferreira *et al.* [259], who investigated lithium insertion behaviour of boron-doped diamond grown on a cloth of graphite fibers, showed that lithium insertion led to $Li_x(B_zC_{1-z})_6$ compositions. They demonstrated a reversible capacity of 88 mAh/g ($x \sim 0.23$) for a sample with 10^{18} B/cm^3 and 43 mAh/g ($x \sim 0.11$) for a sample with 10^{21} B/cm^3. The voltage *vs.* capacity curves showed a hysteresis, which increased with decreasing boron concentration [249]. Christy *et al.* [260] used boron-doped diamond obtained by a HF-CVD method as lithium insertion anode. They reported a capacity of 130 mAh/g with a composite of boron-doped diamond with 2% nanotin. The capacity of the composite represented a jump of 100 mAh/g over that of the HF-CVD derived boron-doped diamond. Considering that the share in the capacity from nanotin cannot exceed the theoretical contribution of 20 mAh/g (for 2% Sn content), the high capacity of the composite looks extraordinary. At any rate, boron-doped diamond with increased number of sp^2 and sp^3 sites with good intercalation kinetics should be considered as a candidate despite its relatively low capacity, for they present large surface areas, possess good thermal and mechanical stabilities, and can be deposited in thin porous forms. It is appropriate to recall at this juncture of the discovery of a new form of carbon whose structure is intermediate between graphite and diamond. This phase has recently been identified as a product formed by a thermobaric treatment of C_{60} and C_{70} molecules [261].

7.2. *Doping with other elements*

Schoenfelder *et al.* [243] reported reversible capacities of up to 450 mAh/g with phosphorus-doped hard carbons; however, their charge-discharge profiles had large hystereses. The nature of bonding in these materials suggest that phosphorus has a softening effect on the structure of hard carbons, and as a result the carbon layers attain more parallel orientations with decreased inter-layer spacings [243]. The hysteresis was attributed to lithium binding to the phosphorus [3].

Chang *et al.* [262] showed that disordered carbons obtained by pyrolyzing a mixture of 3,4,9,10-perylene-tetracaboxylic acid-dianhydride and sulfur exhibited greatly improved capacity and cycling properties. It is believed that the disordered carbon atoms get interconnected by sulfur atoms [263], whose larger covalent diameter (1.02 Å) compared to carbon (0.77 Å) would lead to an increase in the interlayer spacing, favouring easier reversible lithium insertion and maintaining structural stability of the host during cycling.

Nitrogen has also been investigated as a dopant. Wu *et al.* [264], who investigated the lithium insertion properties of nitrogen-containing carbons obtained by carbonization of polyacrylonitrile and melamine–aldehyde resin, found that nitrogen could exist as graphene-nitrogen (nitrogen in the carbon lattice) and as conjugated nitrogen (–C=N). The absence of amino nitrogen would contribute to reduced irreversible capacity. The higher electronegativity of nitrogen (3.5) as compared to carbon (3.0) should result in stronger bonding with lithium [265]. Furthermore, conjugation between the lone-pair electrons in the nitrogen atom and the graphene π-system [266–268] may lead to materials with tailored properties. Wu's group [265] reported capacities as high as 538 mAh/g with nitrogen-doped carbons. Two results were striking in their results: (i) an increase in the temperature of carbonization led to a decrease in the amount of graphene-nitrogen (due to the thermodynamic instability of nitrogen-containing graphene) and (ii) an increase in the reversible capacity with an increase in the graphene-nitrogen content. The study calls into attention the importance of the amount and form in which nitrogen should exist in the carbon in order to realize high reversible capacities. A recent report on the synthesis of nitrogen-doped carbon nanotube cups (also called nanobells) [269,270], containing 2–7% nitrogen and shown to exhibit electrocatalytic activity comparable with that of platinum for the oxygen reduction reaction [271,272], paves the way for more interesting studies with nitrogen-doped carbons especially because unlike nitrogen-doped CNTs or nitrogen-doped graphene, where nitrogen atoms are distributed along the whole surface, they are concentrated on the basal edges of individual cups within the stacked fiber of these nanobells [270]. These nanobells may also be able to store larger amounts of lithium as do curved carbon lattices.

8. Surface modification and irreversible capacity

8.1. *Irreversible capacity*

As noted already, several carbon varieties are limited in their applicability because of large irreversible capacities. Irreversible capacity losses arise due to a number of reasons: formation of an SEI during the first lithiation process (at ~0.8 V *vs.* Li^+/Li) [273–275], irretrievable trapping of lithium in the inner pores of carbon (by electrostatic bonding with surface functional groups through $–COO^-Li^+$ [276] or by reaction with adsorbed oxygen/water molecules [277]. The extent of SEI formation is proportional to the BET surface area of the carbon [278–280], although this correlation is not established with mesoporous carbons such as carbon nanotubes for which the irreversible capacity depends on the volume of mesopores in them [281], where litium is apparently trapped in its metallic state [282]. However, Beguin *et al.* [283,284] suggested that the active surface area (ASA) was a more universal parameter that determines the extent of SEI formation. ASA is a cumulative surface area of different types of defects present on carbon surfaces such as stacking faults, single and multiple vacancies, dislocations, etc. [285]. Thus, deactivation of the carbon surface with a coating of, say, a pyrolytic carbon, can reduce irreversible capacity.

8.2. *Surface-modified graphites*

One disadvantage of graphite as an anode material is its propensity to exfoliate in the presence of electrolytes based on propylene carbonate [176,286–288], a solvent that seems central for low-temperature applications given its low melting point (−49.8°C). The thus exposed surface reduces the electrolyte (releasing potentially explosive propylene [176]), which enhances the irreversible capacity and lowers the coulombic efficiency. This calls for methods to arrest co-intercalation of propylene carbonate into the graphite lattice. Approaches to prevent or diminish intercalation of the solvent, which occurs at potentials of less than 1 V *vs* Li^+/Li [3], have focused on surface modification of graphite. Surface modification has been achieved by several methods including heating under controlled atmospheres [289], mild oxidation [164,290,291], removal of surface oxygen species by high-temperature pumping [292], surface fluorination [293], silylation of surface hydroxyl groups [291], pre-treatment in a polyelectrolyte solution [294] and by use of film-forming additives in the electrolyte [3,295,296].

8.2.1. *Mild oxidation*

Mild oxidation can generate nanochannels or nanopores near the surface, which can lead to an increase in reversible capacity [3,164]. On the other hand, strong oxidation can be pejorative, often resulting in large irreversible capacities. Electrolyte additives should produce SEIs that are selectively permeable to unsolvated lithium ions only, preventing co-intercalation of the solvent. Moreover, the additives should form the SEI at potentials more positive than that at which solvent intercalation occurs. Examples of such additives include chloroethylene carbonate [297] and ethylene sulphite [298]. In the fluorination process, surface oxygen species can get replaced by fluorine. In the first lithiation step, the fluorine can be removed as LiF, which results in a carbon surface with reduced concentration of oxygen-containing species. It has been shown that surface-fluorinated graphites deliver higher reversible capacities [293], sometimes exceeding the theoretical value of graphite [299]. Nakajima [293] suggested an increase in surface roughness and generation of naphthalene- and/or anthracene-like disordered carbons at the surface upon fluorination. It was suggested that lithium formed a charge-transfer complex with the aromatic rings in the surface nanopores, accounting for the large capacities [300].

8.2.2. *Coatings*

Another approach is to coat graphite with a layer of amorphous carbon, which can prevent direct contact of the electrode and the electrolyte. Yoshio *et al.* [15,301,302] used a thermal vapor decomposition technique to coat carbon on natural graphite, and found that the coated graphite not only suppressed electrolyte decomposition but also exhibited excellent lithium insertion properties. However, the solvent-sieving amorphous carbon coating decreases the reactivity of the electrode material. The coating being lower in density (about 1.86 g/cm^3) than graphite (2.27 g/cm^3), there is reduction in electrode density with coating, which can impact on the energy density of the batteries. Yoshio *et al.* [303] also used a core-shell composite of natural graphite in carbon by which they ensured thin coatings and cost reduction. In their new approach [303], the authors folded graphite fragments into a compact ball by impact milling so that a large portion of the edge planes, through which exfoliation takes place, is submerged in the graphite balls. They suggested that the resulting spherical carbon-coated graphites were isotropic, in contrast to the original graphite. Anisotropic graphite particles upon coating would have the basal planes parallel to the current collector, retarding their rate capability [304]; on the other hand, the isotropic spherical carbon-coated graphite should be more favorable for high-drain applications.

Zhang *et al.* [305,306] studied graphite coated with carbon derived from polyvinyl chloride. They showed that it was important to understand the pyrolytic behaviour of the carbon precursor in order to arrive at a coating with appropriate structural and morphological features necessary for optimal electrochemical performance [306]. On the basis of a thermogravimetry–mass spectrometry study, they suggested a multi-step carbonization procedure, which yielded carbon-coated natural graphite with a steady reversible capacity of more than 330 mAh/g [306]. Yang *et al.* [307] demonstrated a specific capacity of as much as 367 mAh/g with natural graphite coated with silica. Compared to natural graphite, which showed a capacity retention of only 83.04% after 40 cycles, the silica-coated graphite showed a capacity retention of 99.55%.

9. Composites

Any discussion on the future of carbon-based anode materials will be incomplete sans carbon-containing composite anodes. Composites are often the only way to maximize performance of the constituent materials. A typical carbon-carbon composite is one with carbon nanotubes bridged with mesoporous carbon particles [308] prepared by depositing ordered mesoporous carbon (OMC) and CNTs sequentially inside the pores and on the external surfaces, respectively, of an SBA-15 template. The composite exhibited enhanced cycling performance and rate capability, although the CNT decoration somewhat lowered the initial capacity of OMC. The improvement in performance was attributed to the higher electrical conductivity of the composite (645 S/cm) as compared to that of OMC (138 S/m). A nanocomposite of CNTs and gold particles in a block copolymer matrix sustained more than 600 cycles at rates varying between C/1.8 and 8.8C [309]. Composites provide necessary resilience to accommodate volume changes that accompany insertion and deinsertion in alloy anodes such as tin and silicon [310]. A matrix of carbon with these elements will also help prevent agglomeration of active particles, thus maintaining active surface area and electrochemical activity. Composites can also enhance electronic conductivity, support improved lithium diffusion and maintain morphological stability. We make no attempt to review the multitude of carbon-based anode materials here. Instead, our attention will be restricted to nanocomposite anode materials, essentially to highlight the novelty in approaches to high-capacity anodes.

9.1. *Carbon-tin composites*

By far the maximum attention has been focused on composites of carbon with tin. This is only natural given the fact that tin exhibits a theoretical capacity of 994 mAh/g (corresponding to a maximum stoichiometry of $Li_{22}Sn_5$), the highest among metals. It also has an active range hovering around 0.3 V *vs.* Li^+/Li. Resort to composite electrodes is made in order to offset internal stress due to volume changes (about 300%) that accompany the lithiation and delithiation processes [311,312]. Coating of tin particles with carbon is accomplished by several ways including mechanical mixing [313,314] and hydrothermal method [314]. However, such composites exhibit capacities between those of carbons and the alloying metal. Investigations on composites of CNTs with tin/tin alloys have also been carried out. Examples include CNT-Sn [315], CNT-Sn_2Sb [316], CNT-SnNi [315] and CNT-AgFeSn [317].

9.1.1. *Tin@carbon hollow spheres*

Tin encapsulated in hollow carbon spheres are of particular interest [318–320]. An important feature of these structures is the void space provided by the carbon sphere within which the alloy anode can freely expand and contract [320–325]. Because tin has a low melting point (232°C), it is difficult to trap tin in a carbon shell formed by pyrolytic processes. Cui *et al.* [326], however, obtained tin-encapsulated carbon by a simple solid-state pyrolysis route with allyltriphenyltin. Compared to similar nanotin-carbon composites, characterized by poor cyclability and capacities of about 450 mAh/g [318], this material gave highly stable capacities of about 550 mAh/g [326].

Figure 19: (a) Cycling behaviour of SnSb-CNT nanocomposite (0.050–1.500 V; 100 mA/g); (b) coulombic efficiency of the SnSb-CNT nanocomposite electrode as a function of cycle number [331].

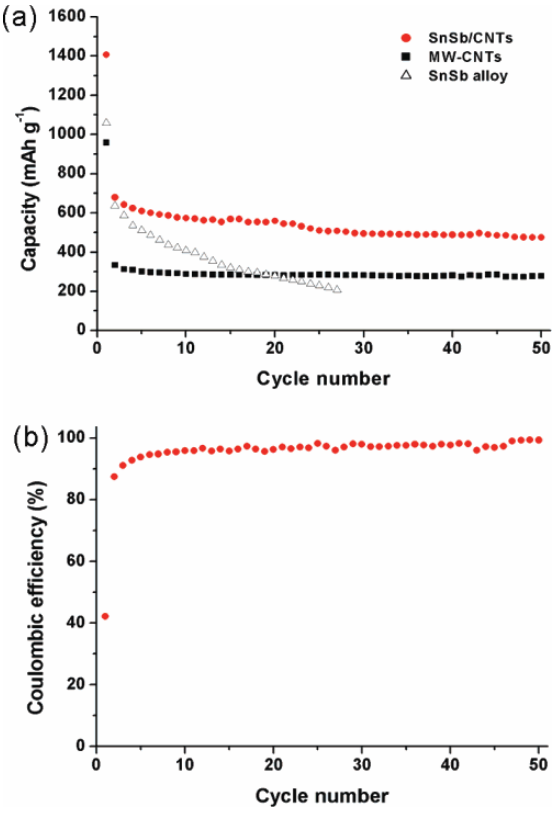

9.1.2. *Tin@carbon nanotubes*

CNTs, with their hollow core, high electrical conductivity and flexibility [327] could also be a good encapsulation matrix. However, a number of CNT-Sn composites reported in the literature have tin particles deposited on the external walls of CNTs [328–331]. Park *et al.* [331] obtained first-cycle lithium insertion and deinsertion capacities of 1,408 and 680 mAh/g with SnSb-CNT nanocomposites (Fig. 19). The deinsertion capacity in the 50th cycle was 480 mAh/g. The good cycling behaviour was attributed to the nanoscale dimension of the SnSb alloy particles (< 50 nm), pinning the alloy particles on the CNT surfaces that hindered agglomeration of SnSb particles, and to the CNT acting as electronic conductor and absorbing volume variation during the electrochemical reactions.

Because CNTs have good chemical stability, and possess high tensile strength (~50 GPa) and shear strength (~500 MPa), incorporation of CNTs must improve the longevity of the anode. An *ab initio* study of the interactions of tin with the inner and outer walls of single-walled CNT based on density functional theory showed that tin encapsulated in CNTs can withstand the colossal volume changes during the alloying process [332]. Tin encapsulation during arc-discharge synthesis of CNTs proved a failure due probably to the high surface tension of liquid tin, which prevents its encapsulation [333]. Other methods, therefore, have to be employed. Kumar *et al.* [334] synthesized Sn@CNT by introducing molten $SnCl_2$ into open MWCNTs followed by reduction of the salt to the metal. Other approaches include introducing a tin salt or oxide into CNTs and subsequently converting the compound into the metal [335,336], and using tin nanowires as a catalyst to grow CNTs [337]. Kumar *et al.* [334] demonstrated metal-filled CNTs as a novel class of high-capacity lithium-insertion anodes. For example, Sn-filled MWCNTs exhibit capacities much higher than the cumulative values that can be expected from the constituents, with first-cycle deinsertion capacities as high as 889

Figure 20: Cycling behaviour of nanotin (40 nm), unopened, opened and tin-filled MWCNTs. Tin-filling was carried out by a hydrothermal method or with $NaBH_4$.

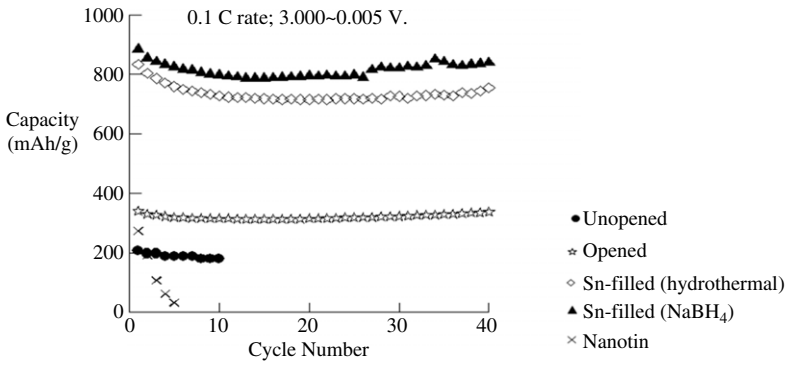

Figure 21: A schematic representation of tin particles in contact with the electronically conducting walls of the carbon nanotube both in the lithiated and delithiated states.

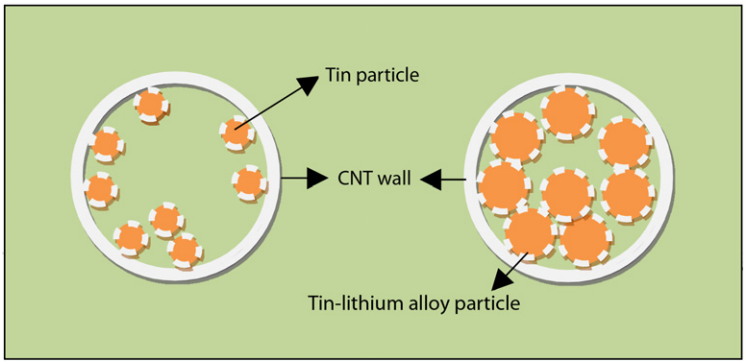

mAh/g (Fig. 20) [334]. The material also sustains extended cycling, which is attributed to (i) the space available in the CNTs for volume expansion during lithiation and (ii) the walls of the CNTs providing an electronically conducting matrix in constant contact with tin both in its lithiated and delithiated states (Fig. 21). However, tin encapsulation was less than 7% by weight. Moreover, the influence of its concentration remains to be investigated. Filling with other metals has also yielded high reversible capacities (Fig. 22) [338]. Chen *et al.* [339] decorated MWCNTs with Sb and $SnSb_{0.5}$ particles and reported reversible capacities of 462 and 528 mAh/g, respectively, for CNT-36 wt% Sb and CNT-56 wt% $SnSb_{0.5}$,composites. The respective capacity fades were 1.3 and 1.1%/cycle over 30 cycles. The high irreversible capacities of metal-filled CNTs and their high cost are deterrents to their commercial exploitation.

Recently, Wang *et al.* [340] reported a templated chemical vapor deposition method by which they produced Sn@CNT with ~100% encapsulation of tin with high filling uniformity. In a modified approach, they also obtained a Sn@C@CNT structure [340]. Charge-discharge studies showed that Sn@CNT and Sn@C@CNT gave initial capacities of 526 and 716 mAh/g, respectively, between 3.000 V and 5 mV. The corresponding first-cycle irreversible capacities were 32.5 and 22.2%.

9.1.3. *Other tin-carbon composites*

Fan *et al.* [341] introduced tin-based oxides into the pores of (ordered mesoporous carbon) CMK-3 nanorod arrays by using a phosphorus ester and obtained an ordered, nanostructured composite, which gave an initial charge capacity of 1,347 mAh/g and subsequently 515 mAh/g. The superiority of the tin oxide/carbon composite was ascribed to a 3-D carbon framework that provided good electronic contact and hindered particle aggregation as well as to confinement of the small grain size of tin-based

Figure 22: Cycling behaviour of bismuth-filled MWCNTs. C/10 rate; 0.005–3.000 V.

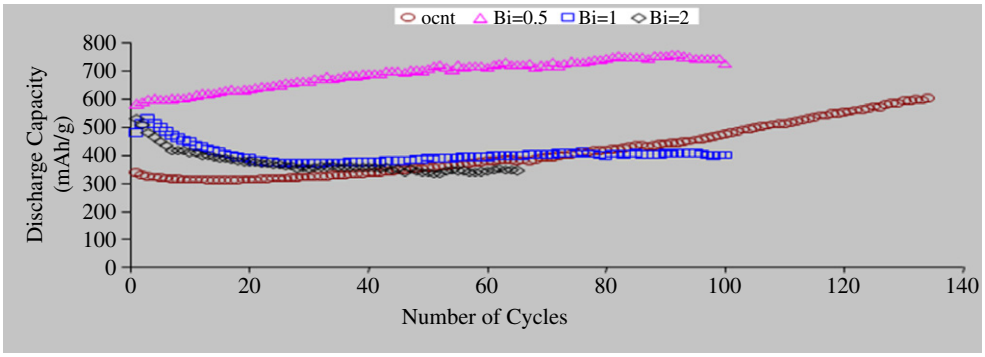

oxides within the nanopores of CMK-3, which prevented formation of two-phase lithium-tin alloys [341].

9.2. *Carbon-silicon composites*

Silicon is considered the ultimate alternative to lithium metal anode owing to its high theoretical capacity (4,200 mAh/g), low cost and abundance on the earth's crust [3,342,343]. However, lithium insertion in silicon is accompanied by an inordinate expansion in volume (400%) [344]. Carbon as a host matrix for silicon nanoparticles is not only conductive but is also ductile [345]. The additional capacity provided by lithium intercalation into carbon will be an added benefit, rendering carbon-silicon composites more attractive. Wang *et al.* [345] demonstrated a first-cycle discharge capacity of about 2,000 mAh/g at C/10 rate with a composite prepared by dispersing nanocrystalline silicon in a carbon aerogel. The material sustained at least 50 subsequent cycles delivering capacities of about 1,450 mAh/g.

9.3. *Metal-metal oxide-carbon nanocomposites*

Special mention must be made of a recent work on the mechanochemical synthesis of and electrochemical lithium insertion studies on a series of metal-metal oxide-carbon nanocomposites. Yoon and Manthiram [346] synthesized Sb-MO_x-C (M = Al, Ti, Mo) nanocomposites synthesized by a mechanochemical reduction of Sb_2O_3 with the respective metal in the presence of acetylene black. The products exhibit excellent lithium insertion properties, with the aluminium-based nanocomposite yielding a first-cycle capacity of 463 mAh/g and more than 430 mAh/g after 100 cycles (Fig. 23). The amorphous metal oxide and the carbon matrix provide the necessary resilience during volume changes that occur upon cycling.

9.4. *Composite conversion anodes*

In a tangential approach from conventional wisdom that considers interstitial-free 3*d*-metal oxides unsuitable for intercalation chemistry and, therefore, untested for rechargeable lithium battery applications, Tarascon *et al.* [347,348] showed that nitrides, fluorides, phosphides, sulphides and borides of 3*d* metals could deliver reversible capacities as large as 1,000 mAh/g. However, their applicability is limited by the large hystereses in their charge–discharge curves [349]. Carbon is used with these materials mainly to improve particle-to-particle electronic conductivity. Lupo *et al.* [350] obtained graphene-covered Co_3O_4 nanoparticles by pyrolysis of cobalt acetylacetonate and subsequent oxidation. The materials gave a reversible capacity of about 940 mAh/g after 20 cycles, which was a substantial improvement over a nano-sized Co_3O_4 sample that rapidly faded to around 120 mAh/g over 20 cycles. The graphene layers are believed to provide both electronic conductivity and buffering action during volume expansion accompanying lithium insertion, thereby enhancing electrochemical performance. In another study aimed at maximizing capacity output by a combination of a soft matrix of carbon nanotubes and the high capacity of Co_3O_4 nanocrystals, Wang *et al.* [351] synthesized CNT/Co_3O_4core-shell one-dimensional nanostructures, which exhibited an initial lithium storage capacity of 1,250 mAh/g and a stable capacity of 530 mAh/g over 100 cycles. NiO as a conversion anode material is also of interest because of its lower cost as compared to cobalt oxides. Good cycling performance has been achieved with Ag-NiO films [352]. Because hollow nanostructures have been found to have lithium insertion properties superior to that of bulk particles [353–355], NiO-based nanotubes are expected to be good lithium-insertion materials. Du *et al.* [356]

Figure 23: Cycling behaviour of Sb-MO_x-C(M = Al, Ti, Mo) nanocomposites (a) C/5 rate at 25°C; (b) C/5 rate at 55°C; (c) at C/5 rate at 25°C at C/5 rate in the presence of 300 ppm Mn^{2+} ions in the electrolyte; and (d) at different rates at 25°C [346].

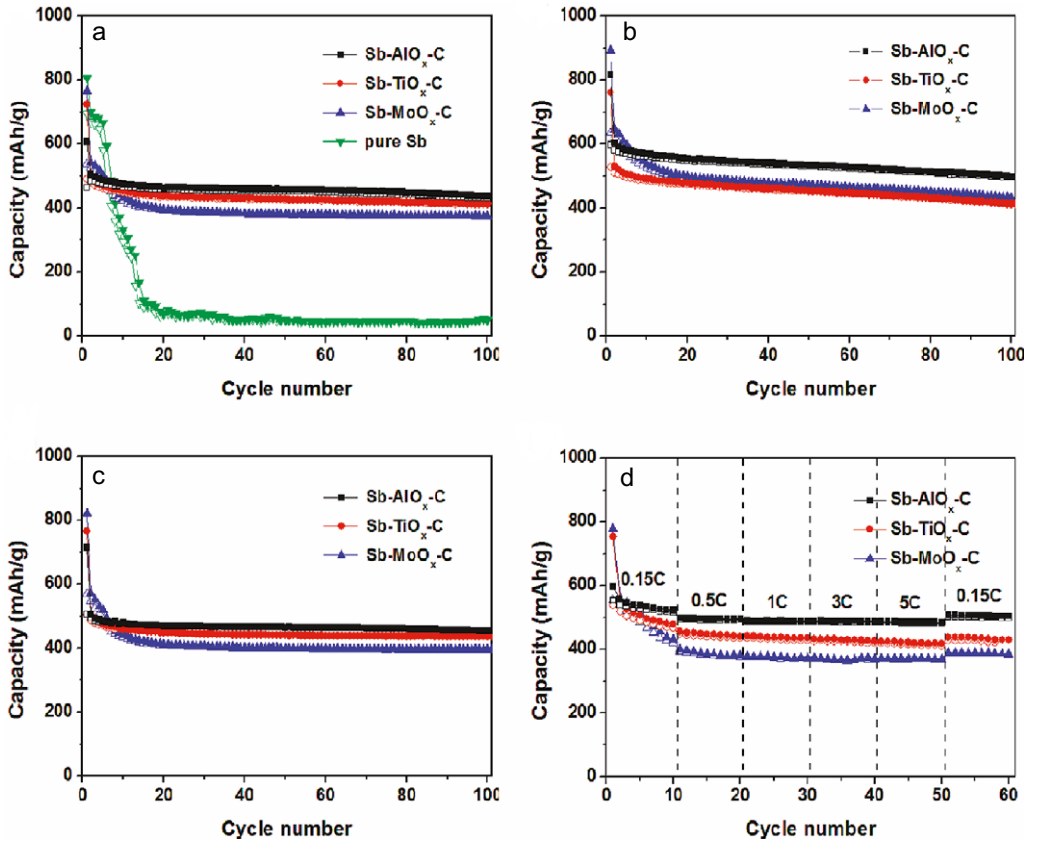

used a layer-by-layer approach for the synthesis of CeO_2-SnO_2-CNT and Ag-NiO-CNT composites with CNT cores. The Ag-NiO-CNT composite gave first-, second- and 20th-cycle capacities of 1305, 845 and 608 mAh/g at a current density of 100 mA/g. It is interesting to note that the 20th-cycle capacity of 608 mAh/g is appreciably higher than that of pure NiO nanotubes (501 mAh/g).

10. Conclusions

The legacy of carbon as an insertion material in lithium-ion batteries is set to continue. Carbonaceous materials continue to amaze us by the sheer variety of their manifestations as by their physical, chemical, mechanical, electrical and thermal properties. This review shows that with a proper understanding of their structure-property relationships, functional carbonaceous materials can be tailored for device applications. We would, however, conclude this review with a caveat—even with cost, abundance and performance on its side, carbon has probably one rival: silicon.

Acknowledgement

Financial assistance for this work under the Inter-Agency Project of the Council of Scientific and Industrial Research, New Delhi is gratefully acknowledged.

Received 27 October 2009; revised 22 December 2009.

References

1. S. Venugopalan, "Lithium-ion cells for space applications," *J. Spacecraft Technol.* 11 (2001) 1–73.
2. T. Nagaura, K. Tozawa, "Lithium ion rechargeable battery," *Prog. Batteries Solar Cells* Vol. 9, JEC Press, Brunswick, OH (1990) 209–217.
3. M. Winter, J.O. Besenhard, M.E. Spahr, P. Novak, "Insertion electrode materials for rechargeable lithium batteries," *Adv. Mater.* 10 (1998) 725–763.
4. M. Armand, J.M. Tarascon, "Building better batteries." *Nature* 451 (2008) 652–657.
5. G.M. Ehrlich, "Lithium-ion batteries," in: Handbook of Batteries, 3rd edn., D. Linden, T.B. Reddy (ed.) McGraw-Hill, New York (2002) pp. 35.1–35.94.
6. T. Prem Kumar, in: The Hindu Speaks on Scientific Facts, Vol. II, Kasturi & Sons, Chennai (2004) pp. 240–242.
7. E. Stura, C. Nicolini, "New nanomaterials for light weight lithium batteries," *Anal. Chim. Acta* 568 (2006) 57–64.

8. E. Peled, "The electrochemical behavior of alkali and alkaline earth metals in nonaqueous battery system – The solid electrolyte interphase model," *J. Electrochem. Soc.* 126 (1979) 2047–2051.
9. M.B. Armand, in: Fast Ion Transport, W. Van Gool (Ed.), North-Holland, Amsterdam (1973) p. 665.
10. T. S. Ong, H. Yang, "Effect of atmosphere on the mechanical milling of natural graphite," *Carbon* 38 (2000) 2077–2085.
11. J.R. Dahn, A.K. Sleigh, H. Shi, J.N. Reimers, Q. Zhong, B.M. Way, "Dependence of the electrochemical intercalation of lithium in carbons on the crystal structure of the carbon," *Electrochim. Acta* 38 (1993) 1179–1191.
12. K. Zaghib, G. Nadeau, K. Kinoshita, "Effect of graphite particle size on irreversible capacity loss," *J. Electrochem. Soc.* 147 (2000) 2110–2115.
13. K. Zaghib, F. Brochu, A. Guerfi, K. Kinoshita, "Effect of particle size on lithium intercalation rates in natural graphite," *J. Power Sources* 103 (2001) 140–146.
14. H.P. Boehm, "Surface oxides on carbon and their analysis: a critical assessment," *Carbon* 40 (2002) 145–149.
15. H. Wang, M. Yoshio, "Carbon-coated natural graphite prepared by thermal vapor decomposition process, a candidate anode material for lithium-ion battery," *J. Power Sources* 93 (2001) 123–129.
16. K. Zaghib, K. Tatsumi, H. Abe, T. Ohsaki, Y. Sawada, S. Higuchi, "Electrochemical behavior of an advanced graphite whisker anodic electrode for lithium-ion rechargeable batteries," *J. Power Sources* 54 (1995) 435–439.
17. M. Fujimoto, Y. Shoji, Y. Kida, R. Ohshita, T. Nohma, K. Nishio, "Influence of solvent species on the charge–discharge characteristics of a natural graphite electrode," *J. Power Sources* 72 (1998) 226–230.
18. Y.A. Kim, M. Kojima, H. Muramatsu, S. Umemoto, T. Watanabe, K. Yoshida, "*In situ* Raman study on single- and double walled carbon nanotubes as a function of lithium insertion," *Small* 2 (2006) 667–676.
19. H. Shi, J. Barker, M.Y. Saıdi, R. Koksbang, L. Morris, "Graphite structure and lithium Intercalation," *J. Power Sources* 68 (1997) 291–295.
20. S. Flandrois, A. Fevrier-Bouvier, K. Guerin, B. Simon, P. Biensan, "On the electrochemical intercalation of lithium into graphitizable carbons," *Mol. Cryst. Liq. Cryst*. 310 (1998) 389–396.
21. C. Lampe-Onnerud, J. Shi, P. Onnerud, R. Chamberlain, B. Barnett, "Benchmark study on high performing carbon anode materials," *J. Power Sources* 97–98 (2001) 133–136.
22. M. Endo, C. Kim, K. Nishimura, T. Fujino, K. Miyashita, "Recent development of carbon materials for Li ion batteries." *Carbon* 38 (2000) 183–197.
23. V.S. Dubasova, A.S. Fialkov, V.L.S. Kanevskii, A. Mikhailova, A.F. Nikolenko, T.A. Ponomareva, S.G. Zaichikov, A.I. Baver, T.Yu. Smirnova, "Electrochemical characteristics of the negative electrode in lithium-ion batteries: Effect of structure and surface properties of the carbon material," *Russ. J. Electrochem*. 40 (2004) 369–378.
24. W.S. Kim, K. Chung, C.B. Lee, J.H. Cho, Y. Sung, Y.K. Choi, "Studies on heat-treated MPCF anodes in Li ion batteries," *Microchem. J*. 72 (2002) 185–192.
25. F. Bonino, S. Brutti, M. Piana, P. Reale, B. Scrosati, L. Gherghel, J. Wu, K. Mullen, "A disordered carbon as a novel anode material in lithium-ion cells," *Adv. Mater*. 17 (2005) 743–746.
26. G.T.K. Fey, C.L. Chen, "High-capacity carbons for lithium-ion batteries prepared from rice husk. *J. Power Sources* 97–98 (2001) 47–51.
27. Y.J. Kim, H.J. Lee, S.W. Lee, B.W. Cho, C.R. Park, "Effects of sulfuric acid treatment on the microstructure and electrochemical performance of a polyacrylonitrile (PAN)-based carbon anode," *Carbon* 43 (2005) 163–169.
28. J.K. Lee, K.W. An, J.B. Jub, B.W. Cho, W. Cho, D. Park, "Electrochemical properties of PAN- based carbon fibers as anodes for rechargeable lithium ion batteries," *Carbon* 39 (2001) 1299–1305.
29. J.B. Gong, H.Q. Wu, Q.H. Yang, "Structural and electrochemical properties of disordered carbon prepared by the pyrolysis of poly(*p*-phenylene) below 1000°C for the anode of a lithium-ion battery," *Carbon* 37 (1999) 1409–1416.
30. W.M. Lu, D.D.L. Chung, "Effect of the pitch-based carbon anode on the capacity loss of lithium- ion secondary battery," *Carbon* 41 (2003) 945–950.
31. H. Imoto, M. Nagamine, Y. Nishi, in: Rechargeable Lithium and Lithium-Ion Batteries, PV 94-28, S. Megahead, B. Barnett, L. Xie (Eds.), The Electrochemical Society, Pennington, New Jersey (1995), p. 43.
32. W. Xing, J.S. Xue, T. Zheng, A. Gibaud, J.R. Dahn, "Correlation between lithium intercalation capacity and microstructure in hard carbons," *J. Electrochem. Soc*. 143 (1996) 3482–3491.
33. H. Azuma, H. Imoto, S. Yamada, K. Sekai, "Advanced carbon anode materials for lithium ion Cells," *J. Power Sources* 81–82 (1999) 1–7.
34. S. Wang, S. Yata, J. Nagano, Y. Okano, H. Kinoshita, H. Kikuta, T. Yamabe, "A new carbonaceous material with large capacity and high efficiency for rechargeable Li-ion batteries," *J. Electrochem. Soc*. 147 (2000) 2498–2502.
35. J.R. Dahn, "Phase diagram of Li_xC_6," *Phys. Rev.* B44 (1991) 9170–9177.
36. Z. Jiang, M. Alamgir, K.M. Abraham, "The electrochemical interaction of Li into graphite in Li/polymer electrolyte/graphite cells," *J. Electrochem. Soc*. 142 (1993) 333–340.
37. M.S. Dresselhaus, G. Dresselhaus, "Intercalation compounds of graphite," *Adv. Phys*. 30 (1981) 139–326.
38. Graphite Intercalation Compounds, Vol. 1 & 2, H. Zabel, S.A. Solin (Eds.), Springer-Verlag, New York (1992).
39. R. Yazami, "Electrode materials based on carbon and graphite intercalation compounds in liquid and polymeric electrolytes," in: Lithium Batteries: New Materials and Perspectives, G. Pistoia (Ed.), Elsevier–North-Holland, New York (1994) pp. 49–91.
40. W.R. McKinnon, R.R. Haering, "Physical mechanism of intercalation," in Modern Aspects of Electrochemistry, Vol. 15, B.E. Conway, R.E. White, J.O'M Bockris (Ed) Plenum Press, New York (1983) pp. 235–304.
41. C. Rigaux, J. Blinowski, "Electronic properties of graphite intercalation compounds," in: Lecture Notes in Physics, Physics of Narrow Gap Semiconductors, Springer Berlin / Heidelberg (1982), pp. 352–362.
42. K. Tatsumi, T. Kawamura, S. Higuchi, H. Hosotubo, H. Nakajima, Y. Sawada, "Anode characteristics of non-graphitizable carbon fibers for rechargeable lithium-ion batteries," *J. Power Sources* 68 (1997) 263–266.
43. K. Tatsumi, T. Akai, T. Imamura, K. Zaghib, N. Iwashita, S. Higuchi, Y. Sawada, "^{7}Li-Nuclear magnetic resonance observation of lithium insertion into mesocarbon microbeads," *J. Electrochem. Soc*. 143 (1996) 1923–1930.
44. D. Fauteux, R. Koksbang, "Rechargeable lithium battery anodes: alternatives to metallic lithium," *J. Appl. Electrochem.* 23 (1993) 1–10.
45. H.H. Landolt, R. Börnstein, Structure Data of the Elements and Intermetallic Phases, Vol. 6, Springer, Berlin (1971).
46. S. Basu, U.S. Pat. 4,304,825 (1981).
47. G.M.T. Foley, C. Zeller, E.R. Falardeau, F.L. Vogel, "Room temperature electrical conductivity of a highly two dimensional synthetic metal: AsF_5-graphite," *Solid State Commun*. 24 (1997) 371–375.
48. F.L. Vogel, G.M.T. Foley, C. Zeller, E.R. Falardeau, J. Gian, "High electrical conductivity in graphite intercalated with acid fluorides," *Mater. Sci. Eng*. 31 (1977) 261–265.
49. T. Tsuzuku, "Anisotropic electrical conduction in relation to

the stacking disorder in graphite," *Carbon* 17 (1979) 293–299.
50. S. Basu, C. Zeller, P. Flanders, C.D. Fuerst, W.D. Johnson, J.E. Fischer, "Synthesis and properties of lithium-graphite intercalation compounds," *Mater. Sci. Eng*. 38 (1979) 275–283.
51. M. Noel, V. Suryanarayanan, "Role of carbon host lattices in Li-ion intercalation/de-intercalation process," *J. Power Sources* 111 (2002) 193–209.
52. J.R. Dahn, T. Zheng, Y. Liu, J.S. Xue, "Mechanisms for lithium insertion in carbonaceous materials," *Science* 270 (1995) 590–593.
53. A.K. Shukla, T. Prem Kumar, "Materials for next-generation lithium batteries," *Curr. Sci*. 94 (2008) 314–331.
54. Y. Yishi, T. Nishida, S. Suda, M. Kobayashi, Hitachi Chemical Company Technical Report 47 (2006) 29.
55. F. Su, X. S. Zhao, Y. Wang, J.H. Zeng, Z.C. Zhou, J.Y. Lee, "Chemical synthesis of graphitic ordered macroporous carbon with a three-dimensional interconnected pore structure for electrochemical applications," *J. Phys. Chem*. B109 (2005) 20200-20206.
56. H. Zhou, S. Zhu, M. Hibino, I. Honma, M. Ichihara, "Lithium storage in ordered mesoporous carbon (CMK-3) with high reversible specific energy capacity and good cycling performance," *Adv. Mater*. 15 (2003) 2107–2111.
57. K.T. Lee, J.C. Lytle, N.S. Ergang, S.M. Oh, A. Stein, "Synthesis and rate performance of monolithic macroporous carbon electrodes for lithium-ion secondary batteries," *Adv. Funct. Mater*. 15 (2005) 547–556.
58. Y.H. Lee, Y.C. Chang, K.C. Pan, S.T. Chang, "The accidental discovery of nature derivative fullerenes developed from DPG," *Mater. Chem. Phys*. 72 (2001) 232–235.
59. Y.H. Lee, K.C. Pan, Y.Y. Lin, V. Subramanian, T. Prem Kumar, G.T.K. Fey, "Graphite with fullerene and filamentous carbon structures formed from iron melt as a lithium-intercalating anode," *Mater. Lett*. 57 (2003) 1113–1119.
60. Y.H. Lee, K.C. Pan, Y.Y. Lin, T. Prem Kumar, G.T.K. Fey, "Lithium intercalation in graphites precipitated from pig iron melts," *Mater. Chem. Phys*. 82 (2003) 750–757.
61. T. Prem Kumar, unpublished results.
62. S. Yata, H. Kinoshita, M. Komori, N. Ando, T. Kashiwamura, T. Harada, K. Tanaka, T. Yamabe, "Structure and properties of deeply Li-doped polyacenic semiconductor materials beyond C_6Li stage," *Synth. Met*. 62 (1994) 153.
63. S. Yata, Y. Hato, H. Kinoshita, N. Ando, A. Anekawa, T. Hashimoto, M. Yamaguchi, K. Tanaka, T. Yamabe, "Characteristics of deeply Li-doped polyacenic semiconductor material and fabrication of a Li secondary battery," *Synth. Met*. 73 (1995) 273.
64. T. Zheng, Y. Liu, E.W. Fuller, S. Tseng, U. von Sacken, J.R. Dahn, "Lithium insertion in high capacity carbonaceous materials," *J. Electrochem. Soc*. 142 (1995) 2581–2590.
65. K. Sato, M. Noguchi, A. Demachi, N. Oki, M. Endo, "A mechanism of lithium storage in disordered carbons," *Science* 264 (1994) 556–558.
66. R. Yazami, M. Deschamps, "High reversible capacity carbon-lithium negative electrode in polymer electrolyte," *J. Power Sources* 54 (1995) 411–415.
67. A. Mabuchi, K. Tokumitsu, H. Fujimoto, T. Kasuh, "Charge-discharge characteristics of the mesocarbon miocrobeads heat-treated at different temperatures," *J. Electrochem. Soc*. 142 (1995) 1041–1046.
68. Y. Liu, J.S. Xue, T. Zheng, J.R. Dahn, "Mechanism of lithium insertion in hard carbons prepared by pyrolysis of epoxy resins," *Carbon* 33 (1996) 193–200.
69. P. Papanak, M. Radosavljevic, J.E. Fischer, "Lithium insertion in disordered carbon-hydrogen alloys: Intercalation *vs* covalent binding," *Chem. Mater*. 8 (1996) 1519–1526.
70. K. Sato, M. Noguchi, A. Demachi, N. Oki, M. Endo, "A mechanism of lithium storage in disordered carbons," *Science* 264 (1994) 556–558.
71. T. Zheng, J.S. Xue, J.R. Dahn, "Lithium insertion in hydrogen-containing carbonaceous materials," *Chem. Mater*. 8 (1996) 389–393.
72. H. Ago, K. Tanaka, T. Yamabe, K. Takegoshi, T. Terao, S. Yata, Y. Hato, N. Ando, "^{7}Li NMR study of Li-doped polyacenic semiconductor (PAS) materials," *Synth. Met*. 89 (1997) 141–147.
73. S. Ishikawa, G. Madjarova, T. Yamabe, "First-principles study of the lithium interaction with polycyclic aromatic hydrocarbons," *J. Phys. Chem*. B105 (2001) 11986–11993.
74. U. Rothlisberger, M.L. Klein, "Determination of the ground state structure and observation of LiH intermediates," *J. Am. Chem. Soc*. 117 (1995) 42–48.
75. H. Ago, M. Kato, K. Yahara, K. Yoshizawa, K. Tanaka, T. Yamabe, "*Ab initio* study on interaction and stability of lithium-doped amorphous carbons," *J. Electrochem. Soc*. 146 (1999) 1262–1269.
76. C. Menachem, E. Peled, L. Burstein, Y. Rosenberg, "Characterization of modified NG7 graphite as an improved anode for lithium-ion batteries," *J. Power Sources* 68 (1997) 277–282.
77. W. Xing, R. Dunlap, J.R. Dahn, „Studies of lithium insertion in ballmilled sugar carbons," *J. Electrochem. Soc.* 145 (1998) 62–70.
78. S. Wang, H. Matsui, H. Tamamura, Y. Matsumura, "Mechanism of lithium insertion into disordered carbon," *Phys. Rev*. B58 (1998) 8163–8165.
79. H. Fujimoto, A. Mabuchi, K. Tokumitsu, T. Kasuh, "Irreversible capacity of lithium secondary battery using meso-carbon micro beads as anode material," *J. Power Sources* 54 (1995) 440–443.
80. K. Tokumitsu, A. Mabuchi, H. Fujimoto, T. Kasuh, "Charge/discharge characteristics of synthetic carbon anode for lithium secondary battery," *J. Power Sources* 54 (1995) 444–447.
81. G. Sandi, R.E. Winans, K.A. Carrado, "New carbon electrodes for secondary lithium batteries," *J. Electrochem. Soc.* 143 (1996) L95–L98.
82. K. Tokumitsu, A. Mabuchi, T. Kasuh, H. Fujimoto, in: Proceedings of the Eighth International Meeting on Lithium Batteries, Nagoya, Japan, 1996, p. 212.
83. E. Peled, C. Menachem, D. Bar-Tow, A. Melman, "Improved graphite anode for lithium-ion batteries chemically bonded solid electrolyte interface and nanochannel formation," *J. Electrochem. Soc*. 143 (1996) L4–L7.
84. R. Setton, P. Bernier, S. Lefrant, Carbon Molecules and Materials, CRC Press, London, 2002.
85. L. Gherghel, C. Kubel, G. Lieser, H. J. Rader, K. Mullen, "Pyrolysis in the mesophase: A chemist's approach toward preparing carbon nano- and microparticles," *J. Am. Chem. Soc*. 124 (2002) 13130–13138.
86. T. Renouard, L. Gherghel, M. Wachtler, F. Bonino, B. Scrosati, R. Nuffer, "Pyrolysis of hexa(phenyl)benzene derivatives: a molecular approach toward carbonaceous materials for Li-ion storage," *J. Power Sources* 139 (2005) 242–249.
87. G.T.K. Fey, D.C. Lee, Y.Y. Lin, "High-capacity carbons prepared from acrylonitrile-butadiene-styrene terpolymer for use as an anode material in lithium-ion batteries," *J. Power Sources* 119–121 (2003) 39–44.
88. F. Bonino, S. Brutti, M. Piana, S. Natale, B. Scrosati, L. Gherghel, K. Mullen, "Structural and electrochemical studies of a hexaphenylbenzene pyrolysed soft carbon as anode material in lithium batteries," *Electrochim. Acta* 51 (2006) 3407–3412.
89. N. Takami, A. Satoh, M. Oguchi, H. Sasaki, T. Ohsaki, "^{7}Li NMR and ESR analysis of lithium storage in a high-capacity perylene-based disordered carbon," *J. Power Sources* 68 (1997) 283–286.
90. G.T.K. Fey, D.C. Lee, Y.Y. Lin, T. Prem Kumar, "High-capacity disordered carbons derived from peanut shells as lithium-

intercalating anode materials," *Synth. Met*. 139 (2003) 71–80.
91. A. Manuel Stephan, T. Prem Kumar, R. Ramesh, S. Thomas, S.K. Jeong, K.S. Nahm, "Pyrolitic carbon from biomass precursors as anode materials for lithium batteries," *Mater. Sci. Eng*. A430 (2006) 132–137.
92. E. Peled, V. Eshkenazi, Y. Rosenberg, "Study of lithium insertion in hard carbon made from cotton wool," *J. Power Sources* 76 (1998) 153–158.
93. K. Tanaka, H. Ago, Y. Matsuura, T. Kuga, T. Yamabe, S. Yata, Y. Hato, N. Ando, "ESR study of Li- doped poly acenic semiconductor (PAS) materials," *Synth. Met*. 89 (1997) 133–139.
94. A. Gibaud, J.S. Xue, J.R. Dahn, "A small angle X-ray scattering study of carbons made from pyrolyzed sugar," *Carbon* 34 (1996) 499–503.
95. G.T.K. Fey, Y.C. Kao, "Synthesis and characterization of pyrolyzed sugar carbons under nitrogen or argon atmospheres as anode materials for lithium-ion batteries," *Mater. Chem. Phys*. 73 (2002) 37–46.
96. G.T.K. Fey, K.L. Chen, Y.C. Chang, "Effects of surface modification on the electrochemical performance of pyrolyzed sugar carbons as anode materials for lithium-ion batteries," *Mater. Chem. Phys*. 76 (2002) 1–6.
97. W. Xing, J.S. Xue, J.R. Dahn, "Optimizing pyrolysis of sugar carbons for use as anode materials in lithium-ion batteries," *J. Electrochem. Soc*. 143 (1996) 3046–3052.
98. J.D. Brooks, G.H. Taylor, "The formation of graphitizing carbons from the liquid phase," *Carbon* 3 (1965) 185–193.
99. I.C. Lewis, "Thermotropic mesophase pitch," *Carbon* 16 (1978) 503.
100. J.L. White, M. Buechler, In: Petroleum Derived Carbons, Vol. 303, J.D. Bacha, J.W. Newman, J.L. White (Eds.), The American Chemical Society, Washington, DC (1986) pp. 62–84.
101. I. Mochida, K. Maeda, K. Takeshida, "Structure of anisotropic spheres obtained in the course of needle coke formation," *Carbon* 15 (1977) 17–23.
102. I. Mochida, Y. Korai , C.H. Kua, F. Watanabe, Y. Sakai, "Chemistry of synthesis, structure, preparation and application of aromatic-derived mesophase pitch," *Carbon* 38 (2000) 305–328.
103. G. Sandi, R.E. Winans, K.A. Carrado, C.S. Johnson, P. Thiyagarajan, "Electrochemical and spectroscopic studies of novel carbonaceous materials used in lithium ion cells," *J. New Mater. Electrochem. Syst.* 1 (1998) 83–89.
104. G. Sandi, K.A. Carrado, R.E. Winans, C.S. Johnson, R. Csencsits, "Carbons for lithium battery applications prepared using sepiolite as inorganic template," *J. Electrochem. Soc*. 146 (1999) 3644–3648.
105. R.E. Gerald II, R.J. Klingler, G. Sandi, C.S. Johnson, L.G. Scanlon, J.W. Rathke, "^{7}Li NMR study of intercalated lithium in curved carbon lattices," *J. Power Sources* 89 (2000) 237–243.
106. C.J. Meyers, S.D. Shah, S.C. Patel, R.M. Sneeringer, C.A. Bessel, N.R. Dollahon, R.A. Leising, E.S. Takeuchi, "Templated synthesis of carbon materials from zeolites (Y, Beta and ZSM-5) and a montmorillonite clay (K 10): Physical and electrochemical characterization," *J. Phys. Chem. B* 105 (2001) 2143–2152.
107. Y.S. Hu, P. Adelhelm, B.M. Smarsly, S. Hore, M. Antonietti, J. Maier, "Synthesis of hierarchically porous carbon monoliths with highly ordered microstructure and their application in rechargeable lithium batteries with high-rate capability," *Adv. Funct. Mater*. 17 (2007) 1873–1878.
108. K. Tanaka, M. Ueda, T. Koike, T. Yamabe, S. Yata, "X-ray diffraction studies of pristine and heavily-doped polyacenic materials," *Synth. Met*. 25 (1988) 265–275.
109. S. Yata, Y. Hato, K. Sakurai, H. Satake, K. Mukai, K. Tanaka, T. Yamabe, "Studies of porous polyacenic semiconductors toward application I. Preparation and structural analysis," *Synth. Met*. 38 (1990) 169–175.
110. A. Herold, "Crystallo-chemistry of carbon intercalation compounds," in: Intercalated Materials, F. Levy (Ed.), Reidel Publishing Company, Dordrecht (1979) pp. 323–421.
111. K. Tanaka, K. Ohzeki, T. Yamabe, S. Yata, "A study on the pristine and the doped polyacenic semiconductive materials", *Synth. Met*. 9 (1984) 41–52.
112. M.C. Suh, Y. Jung, J. Kwak, S.C. Shim, "Structure and electrochemical properties of some synthetic carbons," *Synth. Met*. 100 (1999) 195–204.
113. T. Zheng, Y. Liu, E.W. Fuller, S. Tseng, U. von Sacken, J.R. Dahn, "Lithium insertion in high capacity carbonaceous materials," *J. Electrochem. Soc.* 142 (1995) 2581–2590.
114. N. Takami, A. Satoh, T. Ohsaki, M. Kanda, "Large hysteresis during lithium insertion into and extraction from high capacity disordered carbons," *J. Electrochem. Soc.* 145 (1998) 478–482.
115. L. Zhi, K. Mullen, "A bottom-up approach from molecular nanographenes to unconventional carbon materials," *J. Mater. Chem*. 18 (2008) 1472–1484.
116. S. Mullen, K. Mullen, "Expanding benzene to giant graphenes: towards molecular devices," *Phil. Trans. Royal Soc.* A15 (2007) 1453–1472.
117. C.D. Simpson, G. Mattersteig, K. Martin, L. Gherghel, R.E. Bauer, H.J. Rader, K. Mullen, "Nanosized molecular propellers by cyclodehydrogenation of polyphenylene dendrimers," *J. Am. Chem. Soc*. 126 (2004) 3139–3147.
118. L. Gherghel, C. Kübel, G. Lieser, H.J. Räder, K. Müllen, "Pyrolysis in the mesophase: a chemist's approach toward preparing carbon nano- and microparticles," *J. Am. Chem. Soc.* 124 (2002) 13130–13138.
119. L.G. Scanlon, G. Sandi, "Influence of corannulene's curved carbon lattice ($C_{20}H_{10}$) on lithium intercalation," Proc. 33rd Intersociety Conversion Engineering Conf. (IECEC), Vol. 1, Colorado Springs, CO (1998) p. 223.
120. L.G. Scanlon, G. Sandi, "Lithium-endohedral C_{60} complexes," Proc. 38th Power Sources Conf., Vol. 1, Cherry Hill, NJ (1998) pp. 382–385.
121. N. Kambe, M.S. Dresselhaus, G. Dresselhaus, S. Basu, A.R. McGhie, J.E. Fischer, "Intercalate ordering in first stage graphite-lithium," *Mater. Sci. Eng*. 40 (1979) 1–4.
122. L.G. Scanlon, G. Sandi, "Layered carbon lattices and their influence on the nature of lithium bonding in lithium intercalated carbon anodes," *J. Power Sources* 81–82 (1999) 176–181.
123. J.C. Hanson, C.E. Nordman, "The crystal and molecular structure of corannulene, $C_{20}H_{10}$," *Acta Crystallogr*. B32 (1976) 1147–1153.
124. A.H. Abdourazak, A. Sygula, P.W. Rabideau, "Locking" the bowl-shaped geometry of corannulene: cyclopentacorannulene," *J. Am. Chem. Soc*. 115 (1993) 3010–3011.
125. G. Sandi, R.E. Gerald II, L. Scanlon, C. Johnson, R.J. Klingler, J.W. Rathke, "Molecular orbital and Li-7 NMR investigation of the influence of curved lattices in lithium intercalated carbon anodes,"*J. New Mater. Electrochem. Syst.* 3 (2000) 13–19.
126. W.E. Barth, R.G. Lawton, "Dibenzo[*ghi,mno*]fluoranthene," *J. Am. Chem. Soc*. 88 (1966) 380–381.
127. A. Sygula, P.W. Rabideau, "A practical large scale synthesis of the corannulene system," *J. Am. Chem. Soc*. 122 (2000) 6323–6324.
128. S. Panero, B. Scrosati, M. Wachtler, F. Croce, "Nanotechnology for the progress of lithium batteries R and D," *J. Power Sources* 129 (2004) 90–95.
129. A.S. Aricò, P. Bruce, B. Scrosati, J.M. Tarascon, W.V. Schalkwijk, "Nanostructured materials for advanced energy conversion and storage devices," *Nat. Mater.* 4 (2005) 366–377.
130. H.K. Liu, G.X. Wang, Z.P. Guo, J.Z. Wang, K. Konstantinov, "Nanomaterials for lithium-ion rechargeable batteries," *J.*

Nanosci. Nanotechnol. 6 (2006) 1–15.
131. P.G. Bruce, "Solid-state chemistry of lithium power sources," *Chem. Commun*. 19 (1997) 1817–1824.
132. M. Nishizawa, K. Mukai, S. Kuwabata, C.R. Martin, H. Yoneyama, "Template synthesis of polypyrrole-coated spinel $LiMn_2O_4$ nanotubules and their properties as cathode active materials for lithium batteries," *J. Electrochem. Soc*. 144 (1997) 1923–1927.
133. B.B. Lakshmi, C.J. Patrissi, C.R. Martin, "Sol-gel template synthesis of semiconductor oxide micro- and nanostructures," *Chem. Mater*. 9 (1997) 2544–2550.
134. G. Che, E.R. Fisher, C.R. Martin, "Carbon nanotubule membranes for electrochemical energy storage and production," *Nature* 393 (1998) 346–349.
135. G. Che, B.B. Lakshmi, C.R. Martin, E.R. Fisher, R.A. Ruoff, "Chemical vapor deposition based synthesis of carbon nanotubes and nanofibers using a template method," *Chem. Mater*. 10 (1998) 260–267.
136. G. Che, B.B. Lakshmi, C.R. Martin, E.R. Fisher, "Metal-nanocluster-filled carbon nanotubes: Catalytic properties and possible applications in electrochemical energy storage and production," *Langmuir* 15 (1999) 750–758.
137. R. Moshtev, B. Johnson, "State of the art of commercial Li ion batteries," *J. Power Sources* 91 (2000) 86–91.
138. G. Maurin, F. Henn, B. Simon, J.F. Colomer, J.B. Nagy, "Lithium doping of multiwalled carbon nanotubes produced by catalytic decomposition," *Nano Lett*. 1 (2001) 75–79.
139. I. Mukhopadhyay, N. Hoshino, S. Kawasaki, F. Okino, W.K. Hsu, H. Touhara, "Electrochemical Li insertion in B-doped multiwall carbon nanotubes," *J. Electrochem. Soc*. 149 (2002) A39–A44.
140. B.E. Warren, "X-ray diffraction in random layer lattices," *Phys. Rev*. 59 (1941) 693–698.
141. N.A. Kaskhedikar, J. Maier, "Lithium storage in carbon nanostructures," *Adv. Mater.* 21 (2009) 2664–2680.
142. C.J. Meyers, S.D. Shah, S.C. Patel, R.M. Sneeringer, C.A. Bessel, N.R. Dollahon, R.A. Leising, E.S. Takeuchi, "Templated synthesis of carbon materials from zeolites (Y, Beta, ZSM-5) and montmorillonite clay (K10): Physical and electrochemical characterization," *J. Phys. Chem. B* 105 (2001) 2143–2152.
143. N.C. Li, D.T. Mitchell, K.P. Lee, C.R. Martin, "A nanostructured honeycomb carbon anode," *J. Electrochem. Soc.* 150 (2003) A979–A984.
144. F.Y. Cheng, Z.L. Tao, J. Liang, J. Chen, "Template-directed materials for rechargeable lithium-ion batteries," *Chem. Mater.* 20 (2008) 667–681.
145. D. Dubois, K.M. Kadish, S. Flanagan, L.J. Wilson, "Electrochemical detection of fulleronium and highly reduced fulleride (C_{60}^{5-}) ions in solution," *J. Am. Chem. Soc.* 113 (1991) 7773–7774.
146. Y. Chabre, D. Djurado, M. Armand, W.R. Romanow, N. Coustel, P.J. McCauley, J.E. Fischer, A.B. Smith, "Electrochemical intercalation of lithium into solid fullerene C_{60}," *J. Am. Chem. Soc.* 114 (1992) 764–766.
147. M.S. Dresselhaus, G. Dresselhaus, P.C. Eklund, Science of Fullerenes and Carbon Nanotubes, Academic, San Diego, CA 1996.
148. R.O. Loutfy, S. Katagiri, in: Fullerene Materials for Lithium-ion Battery Applications, E. Osawa (Ed.) Kluwer Academic Publishers, Dordrecht, The Netherlands (2002).
149. T. Kar, J. Pattanayak, S. Scheiner, "Insertion of lithium ions into carbon nanotubes: an *ab initio* study," *J. Phys. Chem.* A 105 (2001) 10397–10403.
150. V. Meunier, J. Kephart, C. Roland, J. Bernholc, "*Ab initio* investigation of lithium diffusion in carbon nanotube systems," *Phys. Rev. Lett.* 88 (2002) 075506-1–4.
151. Y. Liu, H. Yukawa, M. Morinaga, "First-principles study on lithium absorption in carbon nanotubes," *Comput. Mater. Sci.* 30 (2004) 50–56.
152. A. Oberlin, M. Endo, T. Koyama, "Filamentous growth of carbon through benzene decomposition," *J. Cryst. Growth* 32 (1976) 335–349.
153. M. Endo, J. Nakamura, Y. Sasabe, T. Takahashi, M. Inagaki, "Lithium secondary battery using vapor grown carbon fibers as a negative electrode and analysis of the electrode mechanism by TEM observation," *Trans. IEE Jpn*. A115 (1995) 349–456.
154. G.T. Wu, C.S. Wang, X.B. Zhang, H.S. Yang, Z.F. Qi, P.M. He, W.Z. Li, "Structure and lithium insertion properties of carbon nanotubes," *J. Electrochem. Soc*. 146 (1999) 1696–1701.
155. E. Frackowiak, F. Beguin, "Electrochemical storage of energy in carbon nanotubes and nanostructured carbons," *Carbon* 40 (2002) 1775–1787.
156. M. Zhao, Y. Xia, X. Liu, B. Huang, F. Li, Y. Ji, C. Song, "Curvature-induced condensation of lithium confined inside single-walled carbon nanotubes: First-principles calculations," *Phys. Lett*. A340 (2005) 434–439.
157. M. Zhao, Y. Xia, L. Mei, "Diffusion and condensation of lithium atoms in single-walled carbon nanotubes," *Phys. Rev.* B71 (2005) 165413–165459.
158. J. Zhao, A. Buldum, J. Han, "First-principles study of Li intercalated carbon nanotube ropes," *Phys. Rev. Lett*. 85 (2000) 1706–1709.
159. A.S. Claye, J.E. Fischer, C.B. Huffman, A.G. Rinzler, R.E. Smalley, "Solid-state electrochemistry of Li single wall carbon nanotube system," *J. Electrochem. Soc*. 147 (2000) 2845–2852.
160. W. Lu, D.D.L. Chung, "Anodic performance of vapor-derived carbon filaments in lithium-ion secondary battery," *Carbon* 39 (2001) 493–496.
161. H. Shimoda, B. Gao, X.P. Tang, A. Kleinhammes, L. Fleming, Y. Wu, O. Zhou, "Lithium intercalation into opened single-wall carbon nanotubes: storage capacity and electronic properties," *Phys. Rev. Lett*. 88 (2002) 015502-1-4.
162. S.H. Yoon, C.W. Park, H.J. Yang, Y. Korai, I. Mochida, R.T.K. Baker, N.M. Rodriguez, "Novel carbon nanofibers of high graphitization as anodic materials for lithium ion secondary batteries," *Carbon* 42 (2003) 21–32.
163. K. Lin, Y. Xu, G. He, X. Wang, "The kinetic and thermodynamic analysis of Li ion in multi-walled carbon nanotubes," *Mater. Chem. Phys*. 99 (2006) 190–196.
164. T. Prem Kumar, A. Manuel Stephan, P. Thayananth, V. Subramanian, N.G. Renganathan, M. Raghavan, N. Muniyandi, "Thermally oxidized graphites as anodes for lithium-ion cells," *J. Power Sources* 97–98 (2001) 118–121.
165. M. Endo, Y.A. Kim, Y. Fukai, T. Hayashi, M. Terrones, H. Terrones, M.S. Dresselhaus, "Comparison study of semi-crystalline and highly crystalline multiwalled carbon nanotubes," *Appl. Phys. Lett*. 79 (2001) 1531–1533.
166. B. Gao, C. Bower, J.D. Lorentzen, L. Fleming, A. Kleinhammes, X.P. Tang, L.E. McNeil, Y. Wu, O. Zhou, "Enhanced saturation lithium composition in ball-milled single-walled carbon nanotubes," *Chem. Phys. Lett*. 327 (2000) 69–75.
167. I. Mukhopadhyay, S. Kawasaki, F. Okino, A. Govindaraj, C.N.R. Rao, H. Touhara, "Electrochemical Li insertion into single-walled carbon nanotubes prepared by graphite arc-discharge method," *Physica B* 323 (2002) 130–132.
168. S.H. Ng, J.Z. Wang, Z.P. Guo, J. Chen, G.X. Wang, H.K. Liu, "Single wall carbon nanotube paper as anode for lithium-ion battery," *Electrochim. Acta* 51 (2005) 23–28.
169. S.Y. Chew, S.H. Ng, J.Z. Wang, P. Novak, F. Krumeich, S.L. Chou, J. Chen, H.K. Liu, "Flexible free-standing carbon nanotube films for model lithium-ion batteries," *Carbon* 47 (2009) 2976–2983.
170. S. Talapatra, S. Kar, S.K. Pal, R. Vajtai, L. Ci, P. Victor, M.M. Shaijumon, S. Kaur, O. Nalamasu, P.M. Ajayan, "Direct growth of aligned carbon nanotubes on bulk metal," *Nat. Nanotechnol.* 1 (2006) 112–116.
171. Y. Luo, R. Vander Wal, L.J. Hall, D.A. Scherson, "Preparation and characterization of multiwalled carbon nanotubes grown directly onto a conducting support," *Electrochem. Solid- State*

Lett. 6 (2003) A56–A58.
172. J. Chen, A.I. Minett, Y. Liu, C. Lynam, P. Sherrell, C. Wang, G.G. Wallace, "Direct growth of flexible carbon nanotube electrodes," *Adv. Mater*. 20 (2008) 566–570.
173. J. Chen, Y. Liu, A.I. Minett, C. Lynam, J. Wang, G.G. Wallace, "Flexible, aligned carbon nanotubes/conducting polymer electrodes for lithium ion battery," *Chem. Mater*. 19 (2007) 3595–3597.
174. E. Frackowiak, F. Beguin, "Electrochemical storage of energy in carbon nanotubes and nanostructured carbons," *Carbon* 40 (2002) 1775–1787.
175. S.H. Ng, J. Wang, Z.P. Guo, J. Chen, G.X. Wang, H.K. Liu, "Single wall carbon nanotube paper as anode for lithium-ion battery," *Electrochim. Acta* 51 (2005) 23–28.
176. A.N. Dey, B.P. Sullivan, "The electrochemical decomposition of propylene carbonate on graphite," *J. Electrochem. Soc.* 117 (1970) 222–224.
177. G. Eichinger, "Cathodic decomposition reactions of propylene carbonate," *J. Electroanal. Chem*. 74 (1976) 183–193.
178. R. Fong, U. von Sacken, J.R. Dahn, "Studies of lithium intercalation into carbons using nonaqueous electrochemical cells," *J. Electrochem. Soc.* 137 (1990) 2009–2013.
179. B.J. Landi, M.J. Ganter, C.D. Cress, R.A. DiLeo, R.P. Raffaelle, "Carbon nanotubes for lithium ion batteries," *Energy Environ. Sci*. 2 (2009) 638–654.
180. Y. Yang, S. Huang, H. He, A.W.H. Mau, L. Dai, "Pattern growth of well aligned carbon nanotubes; A photolithic approach," *J. Am. Chem. Soc*. 121 (1999) 10832–10833.
181. M. Zhao, H.D. Dewald, R.J. Staniewicz, "Quantitation of the dissolution of battery-grade copper foils in lithium-ion battery electrolytes by flame atomic absorption spectroscopy," *Electrochim. Acta* 49 (2004) 683–689.
182. J. Chen, Y. Liu, A.I. Minett, C. Lynam, J. Wang, G.G. Wallace, "Flexible, aligned carbon nanotube/conducting polymer electrodes for a lithium-ion battery," *Chem. Mater*. 19 (2007) 3595–3597.
183. G. Che, B.B. Lakshmi, E.R. Fisher, C.R. Martin, "Carbon nanotubule membranes for electrochemical energy storage and production," *Nature* 393 (1998) 346–349.
184. B. Gao, A. Kleinhammes, X.P. Tang, C. Bower, L. Fleming, Y. Wu, O. Zhou, "Electrochemical intercalation of single-walled carbon nanotubes with lithium," *Chem. Phys. Lett*. 307 (1999) 153–157.
185. H. Shimoda, B. Gao, X.P. Tang, A. Kleinhammes, L. Fleming, Y. Wu, O. Zhou, "Lithium intercalation into etched single-wall carbon nanotubes," *Physica* B323 (2002) 133–134.
186. M. Khantha, N.A. Cordero, J.A. Alonso, M. Cawkwell, L.A. Girifalco, "Interaction and concerted diffusion of lithium in a (5,5) carbon nanotube," *Phys. Rev.* B78 (2008) 115430-1–9.
187. H. Shimoda, B. Gao, X.P. Tang, A. Kleinhammes, L. Fleming, Y. Wu, O. Zhou, "Lithium intercalation into opened single-wall carbon nanotubes: Storage capacity and electronic properties," *Phys. Rev. Lett.* 88 (2002) 015502-1 –4.
188. J.Y. Eom, H.S. Kwon, "Improved lithium insertion/extraction properties of single-walled carbon nanotubes by high-energy ball milling," *J. Mater. Res.* 23 (2008) 2458–2466.
189. Z.X. Wang, X.D. Wei, T.K. Zhao, Y.N. Liu, "Amorphous carbon nanotubes as new anode material for lithium ion batteries," *Chin. J. Mater. Res.* 22 (2008) 312–316.
190. J. Eom, H.S. Kwon. J. Liu, O. Zhou, "Lithium insertion into purified and etched multi-walled carbon nanotubes synthesized on supported catalysts by thermal CVD," *Carbon* 42 (2004) 2589–2596.
191. M. Endo, C. Kim, T. Karaki, Y. Nishimura, M.J. Matthews, S.D.M. Brown, M.S. Dresselhaus, "Anode performance of a Li ion battery based on graphitized and B-doped milled mesophase pitch-based carbon fibers," *Carbon* 37 (1999) 561–568.
192. C. Kim, T. Fujino, T. Hayashi, M. Endo, M.S. Dresselhaus, "Structural and electrochemical properties of pristine and B-doped materials for the anode of Li-Ion secondary batteries," *J. Electrochem. Soc*. 147 (2000) 1265–1270.
193. Z. Zhou, X.P. Gao, J. Yan, D.Y. Song, M. Morinaga, "Enhanced lithium absorption in single-walled carbon nanotubes by boron doping," *J. Phys. Chem.* B 108 (2004) 9023–9026.
194. Z. Zhou, X.P. Gao, J. Yan, D.Y. Song, M. Morinaga, "A first-principles study of lithium absorption in boron- or nitrogen-doped single-walled carbon nanotubes," *Carbon* 42 (2004) 2677–2688.
195. M. Terrones, W.K. Hsu, S. Ramos, R. Castillo, H. Terrones, "The role of boron nitride in graphite plasma arcs," *Fullerene Sci. Technol*. 6 (1998) 787–800.
196. W.K. Hsu, S. Firth, Ph. Redlich, M. Terrones, Y.Q. Zhu, N. Grobert, A. Schilder, R.J.H. Clark, H.W. Kroto, D.R.M. Walton, "Boron-doping effects in carbon nanotubes," *J. Mater. Chem*. 10 (2000) 1425–1429.
197. D.L. Carrol, Ph. Redlich, X. Blase, J.-C. Charlier, S. Curran, P.M. Ajayan, S. Roth, M. Ruhle, "Effects of nanodomain formation on the electronic structure of doped carbon nanotubes," *Phys. Rev. Lett*. 81 (1998) 2332–2335.
198. B. Wei, R. Spolenak, P. Kohler-Redlich, M. Ruhle, E. Artz, "Electrical transport in pure and boron-doped carbon nanotubes," *Appl. Phys. Lett*. 74 (1999) 3149–3152.
199. B.J. Landi, R.A. DiLeo, C.M. Schauerman, C.D. Cress, M.J. Ganter, R.P. Raffaelle, "Multi-walled carbon nanotube paper anodes for lithium ion batteries," *J. Nanosci. Nanotechnol*. 9 (2009) 3406– 3410.
200. C. Liu, H.M. Cheng, "Carbon nanotubes for clean energy applications," *J. Phys. D: Appl. Phys.* 38 (2005) R231–R252.
201. A.L. Dicks, "The role of carbon in fuel cells," *J. Power Sources* 156 (2006) 128–141.
202. S.H. Yoon, C.W. Park, H. Yang, Y. Korai, I. Mochida, R.T.K. Baker, N.M. Rodriguez, "Novel carbon nanofibers of high graphitization as anodic materials for lithium secondary batteries," *Carbon* 42 (2004) 21–32.
203. G. Zou, D. Zhang, C. Dong, H. Li, K. Xiong, L. Fei, Y. Qian, "Carbon nanofibers: Synthesis, characterization and electrochemical properties," *Carbon* 44 (2006) 828–832.
204. D. Deng, J.Y. Lee, "One-step synthesis of polycrystalline carbon nanofibers with periodic dome- shaped interiors and their reversible lithium-ion storage properties," *Chem. Mater*. 19 (2007) 4198–4204.
205. F. Chevallier, S. Gautier, J.P. Salvetat, C. Clinard, E. Frackowiak, J.N. Rouzaud, F. Beguin, "Effects of post-treatments on the performance of hard carbons in lithium cells," *J. Power Sources* 97–98 (2001) 143–145.
206. E. Buiel, J.R. Dahn, "Li-insertion in hard carbon anode materials for Li-ion batteries," *Electrochim. Acta* 45 (1999) 121–130.
207. J.M. Skowronski, K. Knofczynski, Y. Yamada, "Mechanism of lithium insertion in hollow carbon fibers-based anode," *Solid State Ionics* 157 (2003) 133–138.
208. V. Subramanian, H.W. Zhu, B.Q. Wei, "High rate reversibility anode materials of lithium batteries from vapor-grown carbon nanofibers," *J. Phys. Chem*. B110 (2006) 7178-7183.
209. H.G. Cho, Y.J. Kim, Y.E. Sung, C.R. Park, "The enhanced anodic performance of highly crimped and crystalline nanofibrillar carbon in lithium-ion batteries," *Electrochim. Acta* 53 (2007) 944–950.
210. H. Konno, S. Sato, H. Habazaki, M. Inagaki, "Formation of platelet structure carbon nanofilaments by a template method," *Carbon* 42 (2004) 2756–2759.
211. H. Habazaki, M. Kiriu, H. Konno, "High rate capability of carbon nanofilaments with platelet structure as anode materials for lithium ion batteries," *Electrochem. Commun*. 8 (2006) 1275– 1279.
212. N. Ren, A.G. Dong, W.B. Cai, Y.H. Zhang, W.L. Yang, S.J. Huo, Y. Chen, S.H. Xie, Z. Gao, Y. Tang, "Mesoporous microcapsules with noble metal or noble metal oxide shells and their application in electrocatalysis," *J. Mater. Chem*. 14

(2004) 3548–3552.
213. G.S. Chai, S.B. Yoon, J.H. Kim, J.S. Yu, "Spherical carbon capsules with hollow macroporous core and mesoporous shell structures as a highly efficient catalyst in the direct methanol fuel cell," *Chem. Commun*. (2004) 2766–2767.
214. Y. Xia, R. Mokaya, "Hollow spheres of crystalline porous metal oxides: A generalized synthesis route via nanocasting with mesoporous carbon hollow shells," *J. Mater. Chem*. 15 (2005) 3126–3131.
215. Z. Zhou, Q. Yan, F. Su, X.S. Zhao, "Replicating novel carbon nanostructures with 3D macroporous silica template," *J. Mater. Chem*. 15 (2005) 2569–2574.
216. Y. Wang, F. Su, J.Y. Lee, X.S. Zhao, "Crystalline carbon hollow spheres, crystalline carbon-SnO_2 hollow spheres, and crystalline SnO_2 hollow spheres: Synthesis and performance in reversible Li-ion storage," *Chem. Mater*. 18 (2006) 1347–1353.
217. F. Su, X.S. Zhao, Y. Wang, L. Wang, J.Y. Lee, "Hollow carbon spheres with a controllable shell structure," *J. Mater. Chem*. 16 (2006) 4413–4419.
218. K.T. Lee, J.C. Lytle, N.S. Ergang, S.M. Oh, A. Stein, "Synthesis and rate performance of monolithic macroporous carbon electrodes for lithium-ion secondary batteries," *Adv. Funct. Mater*. 15 (2005) 547–556.
219. S. Ito, T. Murata, M. Hasegawa, Y. Bito, Y. Toyoguchi, "Study on C_xN and C_xS with disordered carbon structure as the anode materials for secondary lithium batteries," *J. Power Sources* 68 (1997) 245–248.
220. T. Nakajima, M. Koh, M. Takashima, "Electrochemical behavior of carbon alloy C_xN prepared by CVD using a nickel catalyst," *Electrochim. Acta* 43 (1998) 883–891.
221. M. Hess, E. Lebraud, A. Levasseur, "Graphite multilayer thin films: a new anode material for Li-ion microbatteries synthesis and characterization," *J. Power Sources* 68 (1997) 204–207.
222. E. Yoo, J. Kim, E. Hosono, H. Zhou, T. Kudo, I. Honma, "Large reversible Li storage of graphene nanosheet families for use in rechargeable lithium ion batteries," *Nano Lett*. 8 (2008) 2277–2282.
223. Y. Matsuo, Y. Suge, "Preparation, structure and electrochemical property of pyrolytic carbon from graphite oxide," *Carbon* 36 (1998) 301–303.
224. T. Szab, O. Berkesi, P. Forg, K. Sepovits, Y. Sanakis, D. Petridis, I. Dkny, "Evolution of surface functional groups in a series of progressively oxidized graphite oxides," *Chem. Mater*. 18 (2006) 2740–2749.
225. S. Wang, P. Chia, L. Chua, L. Zhao, R. Png, S. Sivaramakrishnan, M. Zhou, R. Goh, R.H. Friend, A.T. Wee, P. Ho, "Band-like transport in surface-functionalized highly solution-processable graphene nanosheets," *Adv. Mater*. 20 (2008) 3440–3346.
226. L.R. Radovic, B. Bockrath, "On the chemical nature of graphene edges: Origin of stability and potential for magnetism in carbon matetrials," *J. Am. Chem. Soc*. 127 (2005) 5917–5927.
227. Y. Wang, Y. Huang, Y. Song, X. Zhang, X, Y. Ma, J. Liang, Y. Chen, "Room-temperature ferromagnetism of graphene," *Nano Lett*. 9 (2009) 220–224.
228. D. Pan, S. Wang, B. Zhao, M.H. Wu, H.J. Zhang, Y. Wang, Z. Jiao, "Lithium storage properties of disordered grapheme nanosheets," *Chem. Mater*. 21 (2009) 3136–3142.
229. K.S. Novoselov, A.K. Geim, S.V. Morozov, D. Jiang, Y. Zhang, S.V. Dubonos, I.V. Grigorieva, A.A. Firsov, "Electric field effect in atomically thin carbon films," *Science* 306 (2004) 666–669.
230. C. Berger, Z. Song, X. Li, X. Wu, N. Brown, C. Naud, D. Mayou, T. Li, J. Hass, A.N. Marchenkov, E.H. Conrad, P.N. First, W.A. de Heer, "Electronic confinement and coherence in patterned epitaxial graphene," *Science* 312 (2006) 1191–1196.
231. S. Stankovich, D.A. Dikin, G.H.B. Dommett, K.M. Kohlhaas, E.J. Zimney, E.A. Stach, R.D. Piner, S.T. Nguyen, R.S. Ruoff, "Graphene-based composite materials," *Nature* 442 (2006) 282–286.
232. N. Liu, F. Luo, H. Wu, Y. Liu, C. Zhang, J. Chen, "One-step ionic liquid-assisted electrochemical synthesis of ionic liquid-functionalized graphene sheets directly from graphite," *Adv. Funct. Mater*. 18 (2008) 1518–1525.
233. V.C. Tung, M.J. Allen, Y. Yang, R.B. Kaner, "High-throughput solution processing of large-scale graphene," *Nat. Nanotechnol.* 4 (2009) 25–29.
234. M.A. Hassan, V. Abdelsayed, S.R. Khder, K.M. Abouzeid, J. Terner, M. Samy El-Shall, S.I. Al-Resayes, A.A. El-Azhary, "Microwave synthesis of graphene sheets supporting metal nanocrystals in aqueous and organic media," *J. Mater. Chem*. 19 (2009) 3832–3837.
235. A. Vadivel Murugan, T. Muraliganth, A. Manthiram, "Rapid, facile microwave-solvothermal synthesis of graphene nanosheets and their polyaniline nanocomposites for energy strorage," *Chem. Mater*. 21 (2009) 5004–5006.
236. T. Nakajima, M. Koh, M. Takashima, "Electrochemical behavior of carbon alloy C_xN prepared by CVD using a nickel catalyst," *Electrochim. Acta* 43 (1998) 883–891.
237. A. Marchand, "Electronic properties of doped carbons," *Chem. Phys. Carbon* 7 (1971) 155–191.
238. B.M. Way, J.R. Dahn, "The effect of boron substitution in carbon on the intercalation of lithium in $Li_x(B_zC_{1-z})_6$," *J. Electrochem. Soc*. 141 (1994) 907–912.
239. R. Riedel, "Novel ultrahard materials," *Adv. Mater*. 6 (1994) 549–560.
240. B.M. Way, J.R. Dahn, "The effect of boron substitution in carbon on the intercalation of lithium in $Li_x(B_zC_{1-z})_6$," *J. Electrochem. Soc*. 141 (1994) 907–912.
241. W.J. Weydanz, B.M. Way, T. van Buuren, J.R. Dahn, "Behavior of nitrogen-substituted carbon (N_zC_{1-z}) in Li/Li(N_zC_{1-z})$_6$ cells," *J. Electrochem. Soc*. 141 (1994) 900–907.
242. T.D Tran, J.H. Feikert, S.T. Mayer, X. Song, K. Kinoshita, In: Rechargeable Lithium and Lithium-Ion Batteries, S. Megahed, B.M. Barnett, L. Xie (eds.), The Electrochemical Society, Pennington, NJ (1995) PV94-28, p. 110.
243. H.H. Schönfelder, K. Kitoh, H. Nemoto, "Nanostructure criteria for lithium intercalation in non-doped and phosphorus-doped hard carbons," *J. Power Sources* 68 (1997) 258–262.
244. T.D. Tran, J.H. Feikert, X. Song, K. Kinoshita, "Commercial carbonaceous materials as lithium intercalation anodes," *J. Electrochem. Soc*. 142 (1995) 3297–3302.
245. R.B. Trask, "Effect of boron addition on some properties of synthetic graphite," *Fuel* 47 (1968) 397–402.
246. H.N. Murty, D.L. Biederman, E.A. Heintz, "Apparent catalysis of graphitization. 3 Effect of boron," *Fuel* 56 (1977) 305–312.
247. A. Oya A, R. Yamashita, S. Otani, "Catalytic graphitization of carbons by boron," *Fuel* 58 (1979) 495–500.
248. C.E. Lowell, "Solid solution of boron in graphite," *J. Am. Ceram. Soc*. 50 (1967) 142–144.
249. J.R. Dahn, J.N. Reimers, A.K. Sleigh, T. Tiedje, "Density of states in graphite from electrochemical measurements on $Li_x(C_{1-z}B_z)_6$," *Phys. Rev*. B45 (1992) 3773–3773.
250. B.M. Way, J.R. Dahn, T. Tiedje, K. Myrtle, M. Kasrai, "Preparation and characterization of B_xC_{1-x} thin films with the graphite structure," *Phys. Rev.* B 46 (1992) 1697–1702.
251. P.S. Grosewald, P.L. Walker, Jr., "Effect of boron on the electronic properties of polycrystalline graphite," *Tanso* 61 (1970) 52–59 (In Japanese).
252. J.W. McClure, "Theory of diamagnetism of graphite," *Phys. Rev*. 119 (1960) 606–613.
253. H. Fujimoto, K. Fujiwara, A. Tokumitsu, A. Mabuchi, C. Natarajan, K. Kibata, "Properties of graphite prepared from boron-doped pitch as an anode for rechargeable Li ion battery," Proc. Int. Symp. on Carbon, Chuo University, Tokyo (1998) 308–309.

254. T. Tamaki, T. Kawamura, Y. Yamazaki, "Characteristics of boron doped mesophase pitch-based carbon fibers as anode materials for lithium secondary cells II," Proc. 38th Battery Symp. in Japan, Osaka, Electrochemical Society of Japan (1997) 2B19:257–258.
255. M. Inagaki, H. Konno, T. Tsumura, T. Nakahashi, T. Sogabe, H. Sato, S. Yamaguchi, "Boronated graphites – Chemical state of boron and electrochemical intercalation of lithium," *Trans. Mater. Res. Soc. Japan* 23 (1998) 5–8.
256. U. Tanaka, T. Sogabe, H. Sakagoshi, M. Ito, T. Tojo, "Anode property of boron-doped graphite materials for rechargeable lithium-ion batteries," *Carbon* 39 (2001) 931–936.
257. Y.V. Pleskov, "Electrochemistry of diamond: A review," *Russ. J. Electrochem*. 38 (2002) 1275–1291.
258. K. Patel, K. Hashimoto, A. Fujishima, "Photoelectrochemical investigations on boron-doped chemically vapour-deposited diamond electrodes," *J. Photochem. Photobiol*. A65 (1992) 419–429.
259. N.G. Ferreira, L.L. Mendonca, V.J.T. Airoldi, J.M. Rosolen, "Electrochemical intercalation of lithium into boron-doped CVD diamond electrodes grown on carbon fiber cloths," *Diamond Relat. Mater*. 12 (2003) 596–600.
260. A.Y.M.T. Christy, K.S. Nahm, Y.J. Hwang, E.K. Suh, M.A. Kulandainathan, T. Prem Kumar, A. Manuel Stephan, "Lithium insertion studies on boron-doped diamond as a possible anode material for lithium batteries," *Ionics* 14 (2008) 157–161.
261. V.D. Blank, B.A. Kulnitskiy, Ye.V. Tatyanin, O.M. Zhigalina, "A new phase of carbon," Carbon 37 (1999) 549–554.
262. C.X. Chang, J.F. Xiang, M. Li, X.Y. Han, L.J. Yuan, J.T. Sun, "Improved disordered carbon as high performance anode material for lithium ion battery," *J. Solid State Electrochem*. 13 (2009) 427– 431.
263. X.Y. Han, C.X. Chang, L.J. Yuan, T.L. Sun, J.T. Sun, "Aromatic carbonyl derivative polymers as high-performance Li-ion storage materials," *Adv. Mater*. 19 (2007) 1616–1621.
264. Y.P. Wu, C.Y. Jiang, C.R. Wan, S.B. Fang, Y.Y. Jiang, "Nitrogen-containing polymeric carbon as anode material for lithium ion secondary battery," *J. Appl. Polym. Sci*. 77 (2000) 1735–1741.
265. Y.P. Wu, S.B. Fang, Y.Y. Jiang, "Effects of nitrogen on the carbon anode of a lithium secondary battery," *Solid State Ionics* 120 (1999) 117–123.
266. M. Terrones, H. Terrones, N. Grobert, W.K. Hsu, Y.Q. Zhu, J.P. Hare, H.W. Kroto, D.R.M. Walton, P. Kohler-Redlich, M. Ruhle, J.P. Zhang, A.K. Cheetham, "Efficient route to large arrays of CN_x nanofibers by pyrolysis of ferrocene/melamine mixtures," *Appl. Phys. Lett.* 75 (1999) 3932–3934.
267. W.Q. Han, P. Kohler-Redlich, T. Seeger, F. Ernst, M. Ruhle, N. Grobert, W.K. Hsu, B.H. Chang, Y.Q. Zhu, H.W. Kroto, D.R.M. Walton, M. Terrones, H. Terrones, "Aligned CN_x nanotubes by pyrolysis of ferrocene/C_{60} under NH_3 atmosphere," *Appl. Phys. Lett.* 77 (2000) 1807–1809.
268. X. Wang, X. Li, L. Zhang, Y. Yoon, P.K. Weber, H. Wang, J. Guo, H. Dai, "N-doping of graphene through electrochemical reactions with ammonia," *Science* 324 (2009) 768–771.
269. E.G. Wang, "Review: Nitrogen-induced carbon nanobells and their properties," *J. Mater. Res.* 21 (2006) 2767–2773.
270. B.L. Allen, P.D. Kichambare, A. Star, Synthesis, characterization and manipulation of nitrogen-doped carbon nanotube cups," *ACS Nano* 2 (2008) 1914–1920.
271. K. Gong, F. Du, Z. Xia, M. Durstock, L. Dai, "Nitrogen-doped carbon nanotube arrays with electrocatalytic activity for oxygen reduction," *Science* 323 (2009) 760–764.
272. Y. Tang, B.L. Allen, D.R. Kauffman, A. Star, "Electrocatalytic activity of nitrogen-doped carbon nanotube cups," *J. Am. Chem. Soc.* 131 (2009) 13200–13201.
273. A. Naji, J. Ghanbaja, B. Humbert, P. Willmann, D. Billaud, "Electroreduction of graphite in $LiClO_4$-ethylene carbonate electrolyte. Characterisation of the passivating layer by transmission electron microscopy and Fourier-transform infrared spectroscopy," *J. Power Sources* 63 (1996) 33–39.
274. D. Aurbach, A. Zaban, Y. Ein-Eli, I. Weissman, O. Chusid, B. Markovsky, M. Levi, E. Levi, A. Schechter, E. Granot, "Recent studies on the correlation between surface chemistry, morphology, three-dimensional structures and performance of Li and Li-C intercalation anodes in several important electrolyte systems," *J. Power Sources* 68 (1997) 91–98.
275. K. Kanamura, H. Tamura, S. Shiraishi, Z. Takehara, "Morphology and chemical compositions of surface films of lithium deposited on a Ni substrate in nonaqueous electrolytes," *J. Electroanal. Chem.* 394 (1995) 49–62.
276. D. Larcher, C. Mudalige, M. Gharghouri, J.R. Dahn, "Electrochemical insertion of Li and irreversibility in disordered carbons prepared from oxygen and sulfur-containing pitches," *Electrochim. Acta* 44 (1999) 4069–4072.
277. W. Xing, J.R. Dahn, "Study of irreversible capacities for Li insertion in hard and graphitic carbons," *J. Electrochem. Soc.* 144 (1997) 1195–1201.
278. R. Fong, U. Von Sacken, J.R. Dahn, "Studies of lithium intercalation into carbons using nonaqueous electrochemical cells," *J. Electrochem. Soc*. 137 (1990) 2009–2013.
279. B. Simon, S. Flandrois, A. Fevrier-Bouvier, P. Biensan, "Hexagonal *vs* rhombohedral graphite: The effect of crystal structure on electrochemical intercalation of lithium ions," *Mol. Cryst. Liq. Cryst.* 310 (1998) 333–340.
280. M. Winter, P. Novak, J. Monnier, "Graphites for lithium-ion cells: The correlation of the first-cycle charge loss with the Brunauer-Emmett-Teller surface area," *J. Electrochem. Soc*. 145 (1998) 428–436.
281. E. Frackowiak, F. Béguin, "Electrochemical storage of energy in carbon nanotubes and nanostructured carbons," *Carbon* 40 (2002) 1775–1787.
282. K. Guérin, M. Ménétrier, A. Février-Bouvier, S. Flandrois, B. Simon, P. Biensan, "^{7}Li NMR study of a hard carbon for lithium-ion rechargeable batteries," *Solid State Ionics* 127 (2000) 187–198.
283. F. Béguin, F. Chevallier, C. Vix-Guterl, S. Saadallah, J.N. Rouzaud, E. Frackowiak, "A better understanding of the irreversible lithium insertion mechanisms in disordered carbons," *J. Phys. Chem. Solids* 65 (2004) 211–217.
284. F. Beguin, F. Chevallier, C. Vix-Guterl, S. Saadallah, V. Bertagna, J.N. Rouzaud, E. Frackowiak, "Correlation of the irreversible lithium capacity with the active surface area of modified carbons," *Carbon* 43 (2005) 2160–2167.
285. J. Lahaye, J. Dentzer, P. Soulard, P. Ehrburger, "Carbon gasification: The active site concept," In: Fundamental Issues of Control of Carbon Gasification Reactivity, J. Lahaye, P. Ehrburger (Eds.) Academic Publishers, London (1991), pp. 143–158.
286. M. Arakawa, J. Yamaki, "The cathodic decomposition of propylene carbonate in lithium batteries," *J. Electroanal. Chem*. 219 (1987) 273–280.
287. D. Aurbach, Y. Ein-Eli, O. Chusid, Y. Carmeli, M. Babai, H. Yamin, "The correlation between the surface chemistry and the performance of Li-carbon intercalation anodes for rechargeable 'rocking-chair' type batteries," *J. Electrochem. Soc*. 141 (1994) 603–611.
288. H. Nakamura, H. Komatsu, M. Yoshio, "Suppression of electrochemical decomposition of propylene carbonate at a graphite anode in lithium-ion cells," *J. Power Sources* 62 (1996) 219–222.
289. W. Xing, J.R. Dahn, "Study of irreversible capacities for lithium insertion in hard and graphitic carbons," *J. Electrochem. Soc.* 144 (1997) 1195–1201.
290. J.S. Xue, J.R. Dahn, "Dramatic Effect of oxidation on lithium insertion in carbons made from epoxy resins," *J. Electrochem. Soc.* 142 (1995), 3668–3677.
291. M. Winter, H. Buqa, B. Evers, T. Hodal, K.-C. Moeller, C. Reisinger, M.V. Santis Alvarez, I. Schneider, G.W. Wrodnigg,

F.P. Netzer, R.I.R. Blyth, M.G. Ramsey, P. Golob, F. Hofer, C. Grogger, W. Kern, R. Saf, J.O. Besenhard, "The carbon anode/electrolyte interface in lithium ion cells," *ITE Batt. Lett.* 1–2 (1999) 129–139.
292. T. Takamura, M. Kikuchi. *Battery Technol.* 7 (1995) 29–38.
293. T. Nakajima, "Fluorine-containing energy conversion materials," *J. Fluorine Chem.* 105 (2000) 229–238.
294. M. Gaberscek, M. Bele, J. Drofenik, R. Dominko, S. Pejovnik, "Improved carbon anode for lithium batteries – Pretreatment of carbon particles in a polyelectrolyte solution," *Electrochem. Solid-State Lett.* 3 (2000) 171–173.
295. M. Winter, W. Biberacher, R. Blyth, L.H. Lie, F. Netzer, P. Novák, T. Hodal, M. Ramsey, G.H. Wrodnigg, J.O. Besenhard, Proc. 2nd Hawaii Battery Conf. (1999) p. 215.
296. M. Winter, H. Buqa, B. Evers, T. Hodal, K.-C. Müller, C. Reisinger, M.V. Santis Alvarez, I. Schneider, G.H. Wrodnigg, F.P. Netzer, R.I.R. Blyth, M.G. Ramsey, P. Golob, F. Hofer, C. Grogger, W. Kern, R. Saf, J.O. Besenhard, "The carbon anode / electrolyte interface in lithium ion cells" *ITE Batt. Lett.* 1–2 (1999) 129–139.
297. M. Winter, P. Novák, "Chloroethylene carbonate, a solvent for lithium-ion cells, evolving CO_2 during reduction," *J. Electrochem. Soc.* 145 (1998) L27–L30.
298. G.H. Wrodnigg, J.O. Besenhard, M. Winter, "Ethylene sulfite as electrolyte additive for lithium- ion cells with graphitic anodes," *J. Electrochem. Soc.* 146 (1999) 470–472.
299. T. Nakajima, M. Koh, R.N. Singh, M. Shimada, "Electrochemical behavior of surface-fluorinated graphite," *Electrochim. Acta* 44 (1999) 2879–2888.
300. M. Hara, A. Satoh, N. Takami, T. Ohsaki, "Structural and electrochemical properties of lithiated polymerized aromatics. Anodes for lithium ion cells," *J. Phys. Chem.* 99 (1995) 16338–12343.
301. M. Yoshio, H. Wang, K. Fukuda, Y. Hara, Y. Adachi, "Effect of carbon coating on electrochemical performance of treated natural graphite as lithium-ion battery anode material," *J. Electrochem. Soc.* 147 (2000) 1245–1250.
302. H. Wang, M. Yoshio, T. Abe, Z. Ogumi, "Characterization of carbon-coated natural graphite as a lithium-ion battery anode material," *J. Electrochem. Soc.* 149 (2002) A499–A503.
303. M. Yoshio, H. Wang, K. Fukuda, "Spherical carbon-coated natural graphite as a lithium-ion battery anode material," *Angew. Chem.* 115 (2003) 4335–4338.
304. Z.X. Shu, R.S. McMillan, J.J. Murray, "Electrochemical intercalation of lithium into graphite," *J. Electrochem. Soc.* 140 (1993) 922–927.
305. H.L. Zhang, F. Li, C. Liu, J. Tan, H.M. Cheng, "New insight into the solid electrolyte interphase with use of a focused ion beam," *J. Phys. Chem. B* 47 (2005) 22205–22211.
306. H.L. Zhang, F. Li, C. Liu, H.M. Cheng, "Poly(vinyl chloride) (PVC) coated idea revisited: influence of carbonization procedures on PVC-coated natural graphite as anode materials for lithium ion batteries," *J. Phys. Chem. C* 122 (2008) 7767–7772.
307. Y. Yang, W.J. Peng, H.J. Guo, Z.X. Wang, X.H. Li, Y.Y. Zhou, Y.J. Liu, " Effects of modification on performance of natural graphite coated by SiO_2 for anode of lithium ion batteries," *Trans. Nonferrous Met. Soc. China* 17 (2007) 1339–1342.
308. F. Su, X. Zhao, Y. Wang, J.Y. Lee, "Bridging mesoporous carbon particles with carbon nanotubes," *Micropor. Mesopor. Mater.* 98 (2007) 323–329.
309. S.C. Mui, P.E. Trapa, B. Huang, P.P. Soo, M.I. Lozow, T.C. Wang, R.E. Cohen, A.N. Mansour, S. Mukerjee, A.M. Mayes, D.R. Sadoway, "Block copolymer-templated nanocomposite electrodes for rechargeable lithium batteries," *J. Electrochem. Soc.* 149 (2002) A1610–A1615.
310. C. Cai, Y. Wang, "Novel nanocomposite materials for advanced Li-ion rechargeable batteries," *Materials* 2 (2009) 1205–1238.
311. J.L. Tirado, "Inorganic materials for the negative electrode of lithium-ion batteries: state-of-the-art and future prospects," *Mater. Sci. Eng.* R40 (2003) 103–136.
312. D. Larcher, S. Beattie, M. Morcrette, K. Edstrom, J.C. Jumas, J.M. Tarascon, "Recent findings and prospects in the field of pure metals as negative electrodes for Li-ion batteries," *J. Mater. Chem.* 17 (2007) 3759–3772.
313. T. Morishita, T. Hirabayashi, T. Okuni, N. Ota, M. Inagaki, "Preparation of carbon-coated Sn powders and their loading onto graphite flakes for lithium ion secondary battery," *J. Power Sources* 160 (2006) 638–644.
314. M.J. Noh, Y.J. Kwon, H.J. Lee, J. Cho, Y.J. Kim, M.G. Kim, "Amorphous carbon-coated tin anode material for lithium secondary battery," *Chem. Mater.* 17 (2005) 1926–1929.
315. W.X. Chen, J.Y. Lee, Z. Liu, "The nanocomposites of carbon nanotube with Sb and $SnSb_{0.5}$ as Li- ion battery anodes," *Carbon* 41 (2003) 959–966.
316. Z.P. Guo, Z.W. Zhao, H.K. Liu, S.X. Dou, "Electrochemical lithiation and de-lithiation of MWNT–Sn/SnNi nanocomposites," *Carbon* 43 (2005) 1392–1399.
317. J. Yin, M. Wada, Y. Kitano, S. Tanase, O. Kajita, T. Sakai, "Nanostructured Ag–Fe–Sn/carbon nanotubes composites as anode materials for advanced lithium-ion batteries," *J. Electrochem. Soc.* 152 (2005) A1341–A1346.
318. K.T. Lee, Y.S. Jung, S.M. Oh, "Synthesis of tin-encapsulated spherical hollow carbon for anode material in lithium secondary batteries," *J. Am. Chem. Soc.* 125 (2003) 5652–5653.
319. G. Cui, Y.S. Hu, L. Zhi, D. Wu, I. Lieberwirth, J. Maier, K. Mullen, "A one-step approach towards carbon-encapsulated hollow tin nanoparticles and their application in lithium batteries," *Small* 3 (2007) 2066–2069.
320. W.M. Zhang, J.S. Hu, Y.G. Guo, S.F. Zheng, L.S. Zhong, W.G. Song, L.J. Wan, "Tin- nanoparticles encapsulated in elastic hollow carbon spheres for high-performance anode material in lithium-ion batteries," *Adv. Mater.* 20 (2008) 1160–1165.
321. K.T. Lee, J.C. Lytle, N.S. Ergang, S.M. Oh, A. Stein, "Synthesis and rate performance of monolithic macroporous carbon electrodes for lithium–ion secondary batteries," *Adv. Funct. Mater.* 15 (2005) 547–556.
322. X.W. Lou, Y. Wang, C.L. Yuan, J.Y. Lee, L.A. Archer, "Template-free synthesis of SnO_2 hollow nanostructures with high lithium storage," *Adv. Mater.* 18 (2006) 2325–2329.
323. Y. Wang, H.C. Zeng, J.Y. Lee, "Highly reversible lithium storage in porous SnO_2 nanotubes with coaxially grown carbon nanotube overlayers," *Adv. Mater.* 18 (2006) 645–649.
324. M.S. Park, Y.M. Kang, G.X. Wang, S.X. Dou, H.K. Liu, "The effect of morphological modification on the electrochemical properties of SnO_2 nanomaterials," *Adv. Funct. Mater.* 18 (2008) 455–461.
325. G. Cui, Y.S. Hu, L. Zhi, D. Wu, I. Lieberwirth, J. Maier, K. Mullen, "A one-step approach towards carbon-encapsulated hollow tin nanoparticles and their application in lithium batteries," *Small* 3 (2007) 2066–2069.
326. G. Cui, Y. Hu, L. Zhi, D. Wu, I. Lieberwirth, J. Maier, K. Mullen, "A one-step approach towards carbon-encapsulated hollow tin nanoparticles and their application in lithium batteries," *Small* 3 (2007) 2066–2069.
327. M. Terrones, "Synthesis, properties and applications of carbon nanotubes," *Annu. Rev. Mater. Res.* 33 (2003) 419–501.
328. J. Sloan, J.J. Cook, J.R. Heesom, M.L.H. Green, J.L. Hutchison, "The encapsulation and in situ rearrangement of polycrystalline SnO inside carbon nanotubes," *J. Cryst. Growth* 173 (1997) 81–87.
329. L.P. Zhao, L. Gao, "Filling of multi-walled carbon nanotubes with tin(IV) oxide," *Carbon* 42 (2004) 3269–3272.
330. Z.H. Wen, Q. Wang, Q. Zhang, J.H. Li, "*In situ* growth of mesoporous SnO_2 on multiwalled carbon nanotubes: A novel composite with porous-tube structure as anode for lithium batteries," *Adv. Funct. Mater.* 17 (2007) 2772–2778.
331. M.S. Park, S.A. Needham, G.X. Wang, Y.M. Kang, J.S. Park,

S.X. Dou, H.K. Liu, "Nanostructured SnSb/carbon nanotube composites synthesized by reductive precipitation for lithium-ion batteries," *Chem. Mater.* 19 (2007) 2406–2410.
332. J.W. Zheng, S.M. L. Nai, M.F. Ng, P. Wu, J. Wei, M. Gupta, "DFT study on nano structures of Sn/CNT complex for potential Li-ion battery application," *J. Phys. Chem.* C113 (2009) 14015–14019.
333. C.G. Plecourt, Y.L. Bouar, A. Lolseau, H. Pascard, "Relation between metal electronic structure and morphology of metal compounds inside carbon nanotubes," *Nature* 372 (1994) 761–765.
334. T. Prem Kumar, R. Ramesh, Y.Y. Lin, G.T.K. Fey, "Tin-filled carbon nanotubes as insertion anode materials for lithium-ion batteries," *Electrochem. Commun.* 6 (2004) 520–525.
335. E. Dujardin, T.W. Ebbesen, H. Hiura, K. Tanigaki, "Capillarity and wetting of carbon nanotubes," *Science* 265 (1994) 1850–1852.
336. L. Jankovic, D. Gournis, P.N. Trikalitis, I. Arfaoui, T. Cren, P. Rudolf, M.H. Sage, T.T.M. Palstra, B. Kooi, J.D. Hosson, M.A. Karakassides, K. Dimos, A. Moukarika, T. Bakas, "Carbon nanotubes encapsulating superconducting single-crystalline tin nanowires," *Nano Lett.* 6 (2006) 1131–1135.
337. R.Y. Li, X.C. Sun, X.R. Zhou, M. Cai, X.L. Sun, "Aligned heterostructures of single-crystalline tin nanowires encapsulated in amorphous carbon nanotubes," *J. Phys. Chem.* C111 (2007) 9130–9135.
338. R. Ramesh, T. Prem Kumar, Unpublished results.
339. W.X. Chen, J.Y. Lee, Z.L. Liu, "The nanocomposites of carbon nanotube with Sb and $SnSb_{0.5}$ as Li-ion battery anodes," *Carbon* 41 (2003) 959–966.
340. Y. Wang, M. Wu, Z. Jiao, J.Y. Lee, "Sn@CNT and Sn@C@CNT nanostructures for superior reversible lithium ion storage," *Chem. Mater.* 21 (2009) 3210–3215.
341. J. Fan, T. Wang, C. Yu, B. Tu, Z. Jiang, D. Zhao, "Ordered, nanostructured tin-based oxides/carbon composite as the negative electrode material for lithium-ion batteries," *Adv. Mater.* 16 (2004) 1432–1436.
342. R.A. Sharma, R.N. Seefurth, "Thermodynamic properties of the lithium-silicon system," *J. Electrochem. Soc.* 123 (1976) 1763–1768.
343. B.A. Boukamp, G.C. Lesh, R.A. Huggins, "All-solid lithium electrodes with mixed-conductor matrix," *J. Electrochem. Soc.* 128 (1981) 725–729.
344. H. Li, X.J. Huang, L.Q. Chen, Z.G. Wu, Y. Liang, "A high capacity nano-Si composite anode material for lithium rechargeable batteries," *Electrochem. Solid-State Lett.* 2 (1999) 547–549.
345. G.X. Wang, J.H. Ahn, J. Yao, S. Bewlay, H.K. Liu, "Nanostructured Si–C composite anodes for lithium-ion batteries," *Electrochem. Commun.* 6 (2004) 689–692.
346. S. Yoon, A. Manthiram, "Sb-MOx-C (M = Al, Ti, or Mo) nanocomposite anodes for lithium-ion batteries," *Chem. Mater.* 21 (2009) 3898–3904.
347. P. Poizot, S. Laruelli, S. Grugeon, L. Dupont, J.M. Tarascon, "Nano-sized transition-metal oxides as negative electrode materials for lithium-ion batteries," *Nature* 407 (2000) 496–499.
348. J.M. Tarascon, S. Grugeon, M. Morcrette, S. Laruelle, P. Rozier, P. Poizot, "New concepts for the search of better electrode materials for rechargeable lithium batteries," *C.R. Chim.* 8 (2005) 9–15.
349. P.L. Taberna, S. Mitra, P. Poizot, P. Simon, J.M. Tarascon, "High rate capabilities Fe_3O_4-based Cu nano-architectured electrodes for lithium-ion battery applications," *Nature Mater.* 5 (2006) 567–573.
350. F. Lupo, R. Kamalakaran, A. Gulino, "Viable route for cobalt oxide-carbon nanocomposites," *J. Phys. Chem. C* 113 (2009) 15533–15537.
351. G. Wang, X.P. Shen, J. Yao, D. Wexler, J.H. Ahn, "Hydrothermal synthesis of carbon nanotube/cobalt oxide core-shell one-dimensional nanocomposite and application as an anode material for lithium-ion batteries," *Electrochem. Commun.* 11 (2009) 546–549.
352. X.H. Huang, J.P. Tu, Z.Y. Zeng, J.Y. Xiang, X.B. Zhao, "Nickel foam-supported porous NiO/Ag film electrode for lithium-ion batteries," *J. Electrochem. Soc.* 155 (2008) A438–A441.
353. A.M. Cao, J.S. Hu, H.P. Liang, L.J. Wan, "Self-assembled vanadium pentoxide (V_2O_5) hollow microspheres from nanorods and their Application in lithium-ion batteries," *Angew. Chem. Int. Ed.* 44 (2005) 4391–4395.
354. W.Y. Li, L.N. Xu, J. Chen, "Co_3O_4 nanomaterials in lithium-ion batteries and gas sensors," *Adv. Funct. Mater.* 15 (2005) 851–857.
355. F.S. Cai, G.Y. Zhang, J. Chen, X.L. Gou, H.K. Liu, S.X. Dou, "$Ni(OH)_2$ tubes with mesoscale dimensions as positive electrode materials of alkaline rechargeable batteries," *Angew. Chem. Int. Ed.* 43 (2004) 4212–4216.
356. N. Du, H. Zhang, J.X. Yu, P. Wu, C.X. Zhai, Y.F. Xu, J.Z. Wang, D. Yang, "General layer-by-layer approach to composite nanotubes and their enhanced lithium storage and gas-sensing properties," *Chem. Mater.* 21 (2009) 5264–5271.

Thrivikraman Prem Kumar is a scientist at the Central Electrochemical Research Institute, Karaikudi. He received his MSc (1978) from Loyola College, Chennai and PhD (1989) from the Indian Institute of Science, Bangalore. His research interests are in lithium-based batteries and carbon nanostructures. He may be reached at premlibatt@yahoo.com.

Thanudas Sri Devi Kumari is a research scholar at the Central Electrochemical Research Institute, Karaikudi. She received her MSc (2001) from Holy Cross College, Nagercoil. Her research interests are lithium battery active materials, particularly anodes based on carbon and silicon. She may be contacted at tsp_devi@yahoo.co.in.

Arul Manuel Stephan is a scientist at the Central Electrochemical Research Institute, Karaikudi. He obtained his MSc (1989) from St. Joseph's College, Trichy and PhD (1996) from Alagappa University, Karaikudi. His areas of interest include polymer electrolytes and battery active materials. He may be reached at amanstephan@yahoo.com.